



# A review on the application of benzoxazine as coatings and corrosion inhibitors for corrosion protection of metallic substrates

Roya Malekkhouyan<sup>a,\*</sup>, Marie-Georges Olivier<sup>a,b</sup>

<sup>a</sup> Materials Science Department, Materials Institute, University of Mons, Place Du Parc 20, Mons, 7000, Belgium

<sup>b</sup> Materia Nova Research Center, Parc Initialis, 7000, Mons, Belgium

## ARTICLE INFO

### Keywords:

Benzoxazine  
Bio-based benzoxazine  
Organic coating  
Chemical structure effect  
Corrosion resistance  
Corrosion inhibitor

## ABSTRACT

The global market for benzoxazine resins is expected to grow significantly by 2026, primarily driven by the coatings and composites sectors. These resins are notable for their ability to finely tune the covalent crosslinking of cured systems, which directly influences the properties of the resulting polybenzoxazine for various applications. Understanding the impact of the chemical structure of each precursor on the final polymer properties is essential. Benzoxazines serve as effective coatings and corrosion inhibitors, enhancing the corrosion resistance of metallic substrates exposed to harsh environments. Notably, their application as corrosion inhibitors in acidic media highlights the importance of structural changes on the adsorption energy of the inhibitor molecules. This review summarizes the properties that make benzoxazines suitable for coating applications and discusses various bio-based benzoxazines utilized in these cases. Furthermore, numerous studies have explored the relationship between the chemical structure of benzoxazine monomers and the resulting polybenzoxazines, providing valuable insights into their performance. The information presented in this review is crucial for advancing our understanding and application of benzoxazine resins in protective coatings.

## 1. Introduction

Benzoxazine (Bz) was first introduced by Holly and Cope in 1944. Bz is a molecule composed of an oxazine ring with nitrogen and oxygen heteroatoms in a six-angle ring, and a benzene ring (Fig. 1) [1]. Bz is synthesized from the combination of formaldehyde, primary amines, and phenolic derivatives like phloretic esters [1–3]. Fig. 1 represents schematic formation of Bz monomer and its polymerization in which R, and R<sub>1</sub> can be different functional groups like aliphatic groups. Based on the positions of nitrogen and oxygen atoms within the Bz structure, different isomers of Bz can exist. However, only the 1,3-isomers are capable of forming polybenzoxazine (pBz) [1,4,5].

Using multifunctional amines and phenolic derivatives in the synthesis can produce multifunctional Bz molecules [5,6]. This versatility in molecular design allows Bz to be tailored for various desired properties, such as self-healing, self-cleaning, photo-sensing, and flame retardancy, etc. [1,7–9]. One notable property of Bz is their near-zero shrinkage or volume change during polymerization, which is crucial for their use as coatings and adhesives. The expansion of a polymer upon curing can cause mechanical interlocking to the substrate, while other thermosets like epoxy exhibit high shrinkage, leading to residual stresses that

diminish the coating's protective performance [1,10]. Epoxy coatings have been used extensively in scientific research and industrial applications. However, the curing process results in the formation of micro-cracks, which facilitate the penetration of corrosive ions into the epoxy layer, ultimately reaching the substrate. Therefore, these coatings should be modified with nanomaterials to enhance their protective capabilities [11,12]. Other advantageous properties of pBz include very low surface energy, good thermal and mechanical properties, and hydrophobicity [13–16]. Compared to epoxy, pBzs exhibit rapid physical and mechanical property development at lower molecular weights, while epoxy demonstrates suitable properties at elevated molecular weights and a high degree of conversion [1].

In pBz, complex hydrogen bonding occurs, including both inter and intramolecular OH...OH interactions, intramolecular OH...N interactions (within the oxazine ring), and OH ...  $\pi$  interactions. These hydrogen bonding interactions contribute to the unusual and advantageous properties observed in this polymer [1,17,18]. The stable intramolecular six-membered ring hydrogen bond is responsible for the high modulus, hydrophobicity, low dielectric constant, and high char yield. The ratio of intramolecular to intermolecular hydrogen bonding is dependent on the nature of the amine. Amines with higher pKa values

\* Corresponding author.

E-mail address: [roya.malekkhouyan@umons.ac.be](mailto:roya.malekkhouyan@umons.ac.be) (R. Malekkhouyan).

<https://doi.org/10.1016/j.mtchem.2025.102614>

Received 4 November 2024; Received in revised form 18 February 2025; Accepted 24 February 2025

Available online 6 March 2025

2468-5194/© 2025 Elsevier Ltd. All rights reserved, including those for text and data mining, AI training, and similar technologies.

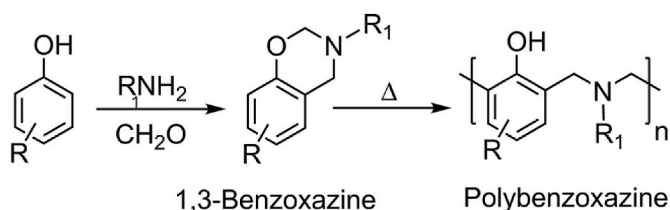


Fig. 1. Synthesis of Bz monomer and the curing process of Bz by ROP, reproduced with permission from Ref. [4].

exhibit a higher intramolecular ratio compared to those with lower pKa values. The majority of the phenolic OH groups form intramolecular hydrogen bonds with N atoms [1].

Bz undergoes ring-opening polymerization (ROP) by heating the monomers within the temperature range of 160–220 °C (Fig. 1) [19]. This polymerization process can occur without the need for strong acids, making Bz suitable for various applications in industrial and academic fields, such as additive manufacturing, membrane, aerospace, electronics, and carbon dioxide adsorption [5,20–29]. It is projected that the global Bz resin market will experience substantial growth in the forthcoming years, with an estimated Compound Annual Growth Rate (CAGR) of approximately 7–8% from 2024 to 2030/2031 [30].

Despite the favorable characteristics of pBz, the purification process for pBz has challenges due to the presence of impurities and solvents [1]. Additionally, pBz exhibits drawbacks such as low cross-linking density, brittleness, and low toughness [5]. These limitations directly impact the suitability of pBz for coating applications, as the material requires a high curing temperature and produces a brittle and breakable film. However, these deficiencies can be mitigated through modifications to the design and structure of the Bz precursors or through the addition of fillers, fibers, and nanoparticles [31–33]. For instance, incorporating functional groups like OH, NH<sub>2</sub>, and CN can reduce the brittleness of pBz [34,35]. Moreover, the toughness of pBz can be enhanced by introducing inorganic fillers to create a composite with improved properties [36]. Another approach involves lowering the curing temperature of Bz by utilizing tertiary amines and excess OH groups, which catalyze and increase transesterification reactions through nucleophilic activation of hydroxyl groups [37]. Furthermore, incorporating long alkyl chains into the chemical structure of precursors can yield liquid and low viscosity Bz at room temperature [38,39]. The adhesion of pBz to metals is facilitated by the interactions between the metal and the phenolic –OH groups, making pBz suitable for coating applications. Additionally, the flexibility of the pBz, resulting from the nature of the polymer backbone, enhances its adhesion to metallic substrates [4]. One notable example of high flexibility is polyester, which contains carboxylic acid and hydroxyl functional groups [40]. Moreover, having longer alkyl chains in the backbone of pBz can increase adhesion due to the flexibility of these chains [3]. However, Bz with mono- or di-functional groups may lead to brittleness and decreased adhesion of the resulting pBz [41]. Higginbottom was the first who developed a cross-linked pBz with a multi-functional Bz for coating applications [42]. As mentioned earlier, the expansion of pBz after curing can enhance adhesion to the substrate and improve corrosion protection. PBz coatings are effective in the corrosion protection of metallic substrates in acidic and saline environments [43–47].

The precursors of Bz often have environmental concerns and are derived from petroleum-based reagents. Moreover, these precursors are challenging to repair or recycle [3,5]. Additionally, when using Bz for coatings, solvents like chloroform are typically employed, which are known to be toxic [3]. Consequently, there is an urge for the production of pBz using more sustainable and environmentally friendly precursors. The production of bio-based materials has gained attention due to their renewable nature and ease of formation [48]. Bio-based Bz can be synthesized by utilizing bio-based compounds and derivatives of amines

and phenols [49,50]. Examples of bio-based amines include furfurylamine [51], dehydroabietylamine [52], stearylamine [53], laurylamine [54]. Similarly, bio-based phenols such as vanillin [55–57], chalcone [58], magnonol [59], eugenol [60,61], sesamol [62,63], chavicol [64], coumarin [65], cardanol [66,67], biphenolic acid, guaiacol, pterostilbene [68] can be used. Bz can also serve as corrosion inhibitors for long-term protection of substrates in acidic environments [69–71]. Corrosion inhibitors are a type of compound used to delay the corrosion of metals by their addition to the corrosive media or coatings [72]. They regulate corrosion behavior in corrosive media by either forming a protective film on the metal surface or altering the double-electrical layer structures [73]. Corrosion inhibitors can be classified into two general groups of inorganic and organic corrosion inhibitors. Chromate, nitrate, phosphate, molybdate, and silicate are among the inorganic corrosion inhibitors used to enhance the corrosion resistance of metallic substrates [70]. However, these inorganic inhibitors have drawbacks, such as reduced tendency to mix with the substrate, non-biodegradability, and environmental issues [70]. Furthermore, inorganic inhibitors exhibit low dispersion in organic coatings which reduces the barrier efficiency provided by the coating [48]. On the other hand, organic inhibitors are composed of compounds that contain multiple bonds, aromatic rings, and hetero-atoms (e.g. nitrogen, oxygen, phosphorus, and sulfur) in their chemical structure [74]. Carboxylate and amine groups in aliphatic compounds have also been found to inhibit corrosion [74]. These heterocyclic compounds, possessing both double bonds and hetero-atoms, have demonstrated exceptional performance in inhibiting corrosion of steel substrates due to their strong affinity for the substrate [70]. The high affinity is related to the strong attraction of hetero-atoms  $\pi$ -electron to the metal empty orbitals, resulting in the formation of a protective layer that prevents further corrosion [48,70]. The inhibition efficiency of these compounds is affected by the size, molecular weight of the organic molecule, aromaticity, number of hetero-atoms and bonding atoms in the molecule, and the nature of corrosive media [71,74]. These factors influence the adsorption efficiency of the organic inhibitor onto the metallic substrate [69]. The inhibition mechanism of organic inhibitors begins with the adsorption of the organic molecules onto the metal surface, followed by their combination with metallic cations to form metal complexes that create a protective layer [69,70,72]. In order to design effective organic inhibitors and identify the active sites of inhibitors for adsorption on the surface, quantum chemical calculations using Density Functional Theory (DFT) can be employed [71].

The inhibition efficiency of corrosion inhibitors or coatings can be calculated using various data. Below, a list of equations utilized for assessing the corrosion inhibition efficiency (E) and corrosion rate (CR) is provided:

$$E(\%) = [(I_{corr} - I_{corr(C)}) / I_{corr}] \times 100 \quad (1)$$

$$CR = (K \times I_{corr} \times EW) / (A \times d) \quad (2)$$

$$CR = (M \times I_{corr}) / (d \times n \times F) \quad (3)$$

$$E(\%) = [(W_0 - W_{inh}) / W_0] \times 100 \quad (4)$$

In these equations,  $I_{corr}$ ,  $I_{corr(C)}$ , K, EW, A, d, n, and F, are corrosion current values of bare and coated samples, corrosion rate constant, equivalent weight of substrate, sample area, density of the substrate, the number of transfer electrons, and Faraday's constant, respectively. In Eq. (4),  $W_0$  and  $W_{inh}$  are weight losses of the substrates in the absence and presence of an inhibitor, respectively. Potentiodynamic polarization measurements are used to determine corrosion current and potential through the analysis of anodic and cathodic slopes in Tafel plots. Generally, a more positive corrosion potential and a lower corrosion current indicate a slower corrosion process [75,76]. Electrochemical impedance spectroscopy (EIS) is a widely used technique for studying

the corrosion protection of organic coatings and the corrosion resistance performance of inhibitors. The Bode and Nyquist diagrams can be obtained from EIS measurements, where systems with a higher impedance modulus at low frequency exhibit higher corrosion resistance [77,78].

This short review provides a concise overview of Bzs that are specifically used for coating applications. In order to address the limitations of traditional pBzs, various approaches have been explored to enhance their applicability in coatings technology. These approaches include: 1) changing the chemical structure of Bz, functionalizing the Bz monomer or copolymerizing it with other Bzs or monomers, and 2) blending it with nanoparticles/nanoplatelets. To comprehensively cover these topics, this review is divided into two sections, each dedicated to summarizing the approaches employed to modify Bzs for use in coating technology. Additionally, the application of Bzs as corrosion inhibitors is discussed in the final section.

## 2. PBz coatings

Polybenzoxazine (pBz) coatings are utilized for passive corrosion protection of metallic substrates, thanks to their excellent thermal and chemical stability, minimal shrinkage, and low surface free energy. To enhance the active corrosion protection of pBz coatings, the Bz monomer can be functionalized with various compounds, such as silane, long alkyl chains, etc. [44]. This section reviews studies on pBz coatings with various molecular designs, pBz functionalized with silane, and those copolymerized with Bz monomers or other monomers for use in coating applications. This versatility allows for achieving desired properties, making the resulting resin suitable for coating applications.

### 2.1. PBz coatings with different molecular designs

The conventional Bz was obtained by the incorporation of bisphenol like bisphenol-A, bisphenol-F, bisphenol-S, and bisphenol-Z [79–81]. Bisphenol-A has been used extensively as the Bz precursor due to its availability, low cost, and high purity [1]. Lu et al. [41] synthesized a bisphenol A-based Bz using the mixture of bisphenol-A, aniline, and paraformaldehyde with a curing temperature of 180 °C for 3h. The coatings were applied on the surface of mild steel (MS) using dip coating method. Comparing the results of obtained pBz coatings with commercial epoxy coating, showed better corrosion protection of pBz coatings (even with lower coating thickness than epoxy coating) due to the more hydrophobic surface of pBz. Hydrophobicity is effective in the long-term corrosion protection of the coatings by creating a barrier layer and isolation for the penetration of corrosive media. Moreover, the effect of monomer concentration and curing temperature of the coatings on the

corrosion protection was investigated. It was observed that increasing the monomer concentration to 500 g/L (increase in the thickness of the coating) and the curing temperature of 180 °C can have the best protection by creating a compact and complete cross-linking network. It has also been demonstrated that elevating the curing temperature above 180 °C increase the volume and thickness of the coatings, thereby reducing their compactness and consequently decreasing their corrosion protection. The epoxy coating was employed as a reference to evaluate the corrosion protection performance of the pBz coating. When both coatings were prepared using the same amount of monomer concentration of 500 g/L, the pBz coating exhibited a lower corrosion current density (obtained from potentiodynamic polarization), with a value of  $4.36 \times 10^{-3} \mu\text{A cm}^{-2}$  compared to  $1.68 \times 10^{-2} \mu\text{A cm}^{-2}$  for the epoxy coating, representing the better performance of pBz coating [41].

The toxicity of bisphenol-A can have significant risks to both human and marine life when employed as a coating in marine applications [82]. Some studies have replaced bisphenol-A with bisphenol-F; however, due to their similar chemical structures, it is likely that they pose similar hazardous effects [83,84]. The chemical structure of different bisphenols is presented in Fig. 2(a) and (b). One of the substituents for these toxic bisphenols is pyrazolidine bisphenol [85]. In their study, Manoj et al. [85] utilized pyrazolidine bisphenol in combination with various amines to synthesize Bz (Fig. 2(c)). The resulting Bzs exhibited lower curing temperatures (approximately 30–50 °C) compared to bisphenol-F-based Bz. Additionally, they demonstrated enhanced corrosion protection and thermal stability. Furthermore, a comparison among different amines revealed that octadecylamine, due to its octadecyl chain, exhibited higher hydrophobicity and more efficient corrosion protection (with an efficiency of 90 %, as determined from corrosion current densities obtained from Tafel plots) than pBz with dodecyl chain or 4-fluoroaryl chain in dodecylamine and 4-fluoroaniline, respectively which was confirmed using polarization and EIS studies. Krishnan et al. [86] developed a bisphenol-F-based Bz by incorporating silane functional groups, aiming to utilize it as a coating for the protection of MS substrates. Comparing results show that adding silane functionality to the chemical structure of pBz coating increased corrosion protection in comparison to conventional bisphenol-based pBz coatings. A high corrosion protection efficiency was reported for the silane-bisphenol pBz coating with the value of 96 %. A comparison of the corrosion rates between bisphenol-A-based and silane-bisphenol-F-based pBz coatings with almost the same thickness reveals a lower corrosion rate with the addition of silane functionality with values of  $5.07 \times 10^{-5} \text{ mm/year}$  and  $3.68 \times 10^{-7} \text{ mm/year}$ , respectively [41,86].

PBz coatings were also employed to protect against the corrosion of

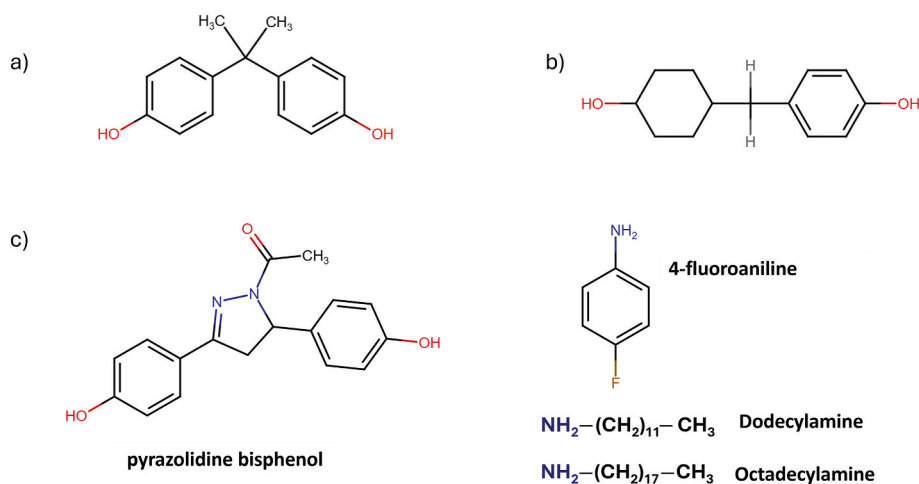


Fig. 2. The chemical structure of a) bisphenol A, b) bisphenol F, and c) synthesis of Bz monomer using pyrazolidine bisphenol and different amines, reproduced based on Ref. [85].

aluminium (Al) substrates. Conventional pBz coatings with bisphenol-A were used for corrosion protection of 1050 Al alloy [87]. Renaud et al. [88] applied Phenol-paraPhenyleneDiAmine (P-pPDA) Bz on sulfo-tartaric anodized Al alloy. In order to avoid the high curing temperature of this Bz, a partial curing at a lower temperature was performed with different temperature cycles. Moreover, the combination of Al alloy anodization and Bz resin could enhance the corrosion protection of the coatings by increasing the cohesive interface between the anodic coating and the substrate. In another study, they used 4-Ethylphenol to obtain 4-ethylphenol-para-phenylenediamine (4 EP-pPDA) [89]. Different curing cycles were performed to reduce the curing temperature. It was observed that corrosion protection is highly influenced by thermal treatment and partial curing of the coating system can compensate for the high curing temperature of Bz which makes them suitable for thermal-sensitive alloys like Al.

Van Renterghem et al. [3] used phloretic acid, ethanolamine, and different diols (dodecandiol (DD)/PEG200/ethylene glycol (EG)) for the synthesis of Bz to investigate the effect of diols backbone in the self-healing and recycling properties. The use of phloretic acid derived from coumaric acid or apple tree leaves by-product, as well as long flexible chains such as alkyl or ether alkyl in the precursors were found to decrease the viscosity and enhance fluidity at room temperature. The excess of the hydroxyl group in ethanolamine helped the transesterification reaction and lowered the curing temperature. Comparing the long-chain effect of dodecandiol and ethylene glycol showed that the longer chain could increase hydrophobicity, self-healing, and corrosion protection (1050 Al alloy) due to the flexibility of the chain, which facilitates the transesterification reaction. The polarity of the PEG and the short chain of ethylene glycol decreased the self-healing ability of these polymers [3]. The coatings were applied on the Al alloy using a bar-coater without the incorporation of solvent. They used commercial epoxy as a reference, observing that after 50 days of immersion in saline solution, the impedance modulus at the low frequency of 0.01 Hz (obtained from EIS results) was  $1 \times 10^{10} \Omega \text{ cm}^2$  for the sample with dodecandiol and  $6.5 \times 10^9 \Omega \text{ cm}^2$  for the commercial epoxy, representing superior corrosion protection for pBz coatings on Al alloys. A comparison of the results for pBz coatings on Al alloys indicates that the impedance modulus at 0.01 Hz was in order of  $10^8 \Omega \text{ cm}^2$  after 30 days of immersion for the conventional pBz coating (the one containing bisphenol-A) with a thickness around 10  $\mu\text{m}$  and in order of  $10^6 \Omega \text{ cm}^2$  after 21 days for P-pPDA with a thickness around 4  $\mu\text{m}$  [87,88]. In the case of pBz with dodecandiol, despite their higher thickness, the corrosion resistance remained sufficiently high, maintaining corrosion protection properties for up to 50 days with an impedance modulus value of around  $10^{10} \Omega \text{ cm}^2$  [3].

Aromatic polyimides have proper properties like high mechanical and thermal properties that can be related to their inert imide ring, which can create strong intermolecular interactions [90,91]. Phthalimide-functionalized (as aromatic polyimides) Bz monomers are effective in anti-corrosive coatings in saline and acidic solutions [45,92]. Fig. 3(a), (b) shows para- and ortho-phthalimide-functionalized used for the synthesis of Bz monomer, referred to as pPP and oPP, respectively. These coatings exhibit hydrophobic properties and a robust cross-linked network structure, thereby minimizing the penetration of the electrolyte. A comparison of these two coatings revealed that the pPP coating, cured at the optimum temperature of 180 °C, provided better corrosion protection, achieving an efficiency of 98 %, compared to 95 % for the oPP coating. The enhanced corrosion protection of the pPP coating is attributed to its stronger coordinate bonding with the substrate [45].

Li et al. [93] investigated the effect of hydrogen bonding on the corrosion protection of pBz coatings by incorporating the phenoxy group in the structure of Bz (Fig. 3(d)). The phenolic sources used in this study are shown in Fig. 3(c) and (d). It is fundamentally expected that the monomer and the polymer that contain the phenoxy group are more hydrophilic and expected to have the penetration of water and, hence, weaker corrosion protection. However, they observed higher corrosion

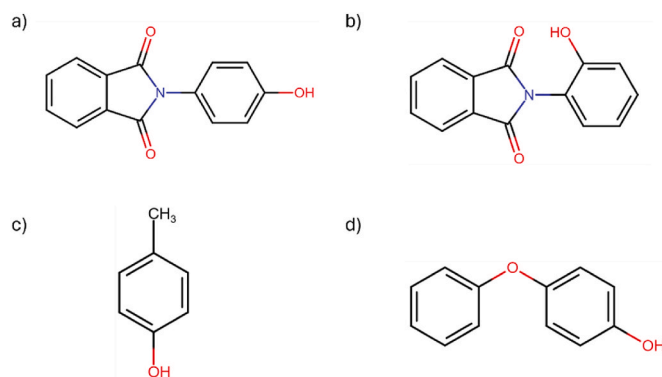


**Fig. 3.** a) Para- and b) ortho-phthalimide-functionalized phenols used for synthesis of Bz monomer, reproduced based on Ref. [45]. Using c) methyl (p-cresol), and d) phenoxy (4-phenoxyphenol) groups for the synthesis of Bz monomer to check the effect of hydrogen bonding on the corrosion protection of pBz coatings, reproduced based on Ref. [93].

protection in the case of having a phenoxy group that is related to the special hydrogen bonding in the structure of pBz coatings. The reason is the steric hindrance caused by the phenoxy group that induced hydrogen atoms in the phenolic hydroxyl group to interact with nitrogen and hydrogen atoms in another phenolic group. So, it can be concluded that having more intramolecular hydrogen bonds than intermolecular bonds is influential for having a more hydrophobic coating and, therefore, better corrosion protection (the amount of the intra- and intermolecular hydrogen bonding was assessed by FTIR [93,94].

In another study, a thymol-based Bz was synthesized according to Fig. 4, using primary amines with different chain lengths (partially bio-based Bz) [49]. The anti-corrosion properties of the obtained coatings were investigated on stainless steel substrates (SS304). It was observed that the hydrophobicity of the coatings increases with increasing the number of carbons in primary amines and also with increasing curing temperature [49,95]. Moreover, better corrosion protection of the coatings with longer amine chains and higher curing temperatures was observed. It was also noted that the corrosion current density of the pBz coating with the longer alkyl chain (T-b in Fig. 4) is almost 55 times less than the pBz with the shorter alkyl chain (T-m in Fig. 4) with an anti-corrosion efficiency of 99.99 %. Increasing the curing temperature (from 160 to 200 °C for 1h) can enhance the complete curing of pBz and the formation of this coating [49].

Furfural bis-thymol, five different fluorinated amines, and para-formaldehyde were utilized to synthesize Bz, which was subsequently applied as a coating on MS substrate [96]. The study demonstrated that increasing fluorine content led to a higher water contact angle, reaching a maximum value of 151°. Furthermore, the incorporation of fluorine in the coating structure significantly enhanced corrosion resistance, which was attributed to the improved cross-linking capability facilitated by fluorine atoms in the amine moieties. The coating efficiencies ranged up to 99 %, with the highest efficiency of 99.99 % observed for the coating containing the highest fluorine content [96].

Srinivasan et al. [97] used trihydroxytriphenylmethane (TTM) with three different amines (1-(3-aminopropyl)imidazole (ipa), dimethylaminopropylamine (dmapa), and aminoethoxyethanol (aee)) that were rich in nitrogen atoms in the backbone of the amine chemical structure to reduce the curing temperature of Bz monomer (Fig. 5(a)). The coatings were applied using spraying over the surface of mild steel (MS). The lowest curing temperature was observed for TTM-dmapa and curing was initiated at 131 °C. This can be related to the accelerated curing process induced by N,N-dimethyl group. Moreover, the more basic nature of amine makes it keener to donate electron pairs that consequently can cleave the oxazine ring in the curing process. TTM-dmapa showed the highest thermal stability with char yield and  $T_{\text{max}}$  ( $T_{\text{max}}$  is defined as the maximum temperature required for pBz degradation) value of 48 % and

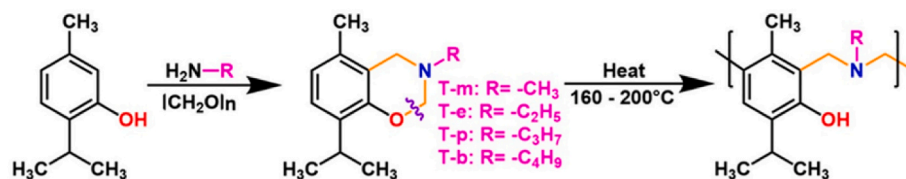


Fig. 4. The synthesis procedure of thymol-based Bz monomer using different amines and the ROP reaction, reproduced with permission from Ref. [49].

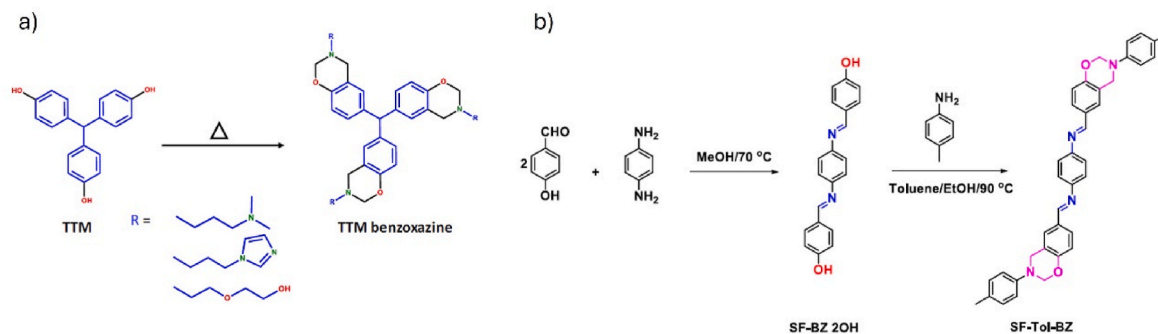


Fig. 5. a) Synthesis of trihydroxytriphenylmethane-based pBz, reproduced with permission from Ref. [97]. b) Schiff base BZ monomer (with p-toluidine) (SF-Tol-BZ), reproduced with permission from Ref. [44].

539 °C, respectively. This sample also had the highest water contact angle with a value of 146°, caused by N,N-dimethyl group as well as aromatic groups in TTM chemical structure. The reason for the stable coatings obtained with these monomers is the highly cross-linked and three-dimensional network, which could enhance the corrosion protection performance of the coating with a corrosion current value of  $5 \times 10^{-12}$  mA (results from potentiodynamic polarization and Tafel studies) and corrosion inhibition efficiency of 99.9 % (Eq. (1)) [98].

Schiff base moiety can be added to the structure of Bz (Fig. 5(b)) to produce a corrosion-protective coating for MS [44]. Schiff bases materials have the ability to be absorbed on the metallic substrate, which makes them suitable for their usage in coating applications [99]. The obtained pBz with Schiff base moieties showed proper thermal stability and corrosion protection and they could decrease the curing temperature of Bz as the ROP is catalyzed by Schiff moieties. The corrosion protection obtained by Schiff base moiety can be due to the adsorption of the coating's molecules onto the MS surface, which was affected by the  $\text{C}=\text{N}$ -, and  $\text{OH}$  phenolic groups of the functional groups. Moreover, these molecules can form a MS-coating complex with the  $\text{Fe}^{2+}$  cations coming from the substrate [44]. The reactions leading to the final Bz monomer is illustrated in Fig. 5(b). Using n-hexylamine Schiff base condensation reaction with salicylaldehyde and further reduction of Schiff base compound with sodium borohydride, a new Bz monomer can be synthesized [43]. The resulting coating can be used for corrosion protection of MS in an acidic solution (0.1 M  $\text{H}_2\text{SO}_4$ ) that is related to the hexyl group in the pBz chemical structure [43].

Bi- and tri-valent nitrogen-rich Schiff bases were synthesized using hydroxynaphthaldehyde in combination with acetoguanamine (AG), benzoguanamine (BG), and melamine (MA) to serve as phenolic sources for Bz synthesis [100]. These Schiff bases were subsequently used with furfurylamine and paraformaldehyde to produce Bz monomers. The resulting coatings demonstrated an inhibition efficiency of 99 %, effectively protecting MS from corrosion. The corrosion protection properties are attributed to the abundant nitrogen content, the presence of imine groups, and their inherent corrosion resistance. Additionally, the strong adhesion of the coatings to the substrate, along with their hydrophobic nature, significantly contributes to their protective performance. Among the coatings, the one derived from MA exhibited the highest hydrophobicity (145°), attributed to its nitrogen-rich rigid aromatic core, which minimizes interactions between the coating and water

molecules.

Muthukumar et al. [101] used curcumin with three different primary amine: octadecylamine, aniline, and furfurylamine, and the usage of bio-based Bz was confirmed for coating applications and corrosion protection of MS. The corrosion protection provided by the pBz coating derived from furfurylamine was the highest, with a corrosion inhibition efficiency of 99.6 % using the Tafel curve of potentiodynamic polarization test (Eq. (1)), primarily attributed to the presence of a cross-linked network and the polar characteristics of the monomer, which enhances the adhesion of the coating to the MS substrate. The existence of an aliphatic chain in the structure of the pBz coating with octadecylamine contributed to the highest water contact angle for this sample. However, for this sample, corrosion protection was the lowest, with a corrosion inhibition efficiency of 98 % (Eq. (1)). Therefore, it can be concluded that the improved adhesion resulting from the incorporation of furfurylamine into the pBz coating structure contributes more significantly to enhancing corrosion protection performance than the increased hydrophobicity provided by the long aliphatic chain of octadecylamine (water contact angles for pBz coating with octadecylamine and furfurylamine are 137° and 135°, respectively) [101]. Curcumin as well as its combination with chitosan was also used for the synthesis of pBz to inhibit corrosion and biofilm formation in which the Bz monomer was synthesized by Schiff base chemistry [102,103]. Chitosan as a biopolymer that is obtained from the shells of crustaceans, can be blended with Bz to increase the mechanical, thermal, and antimicrobial characteristics [103].

Curcumin has been used with other amines including adamantylamine (adm), aniline (a), allyl amine (aa), amino ethoxyethanol (aee), amino propyl imidazole (api) and trifluoro methyl aniline (tfma) for the synthesis of Bz [104]. Comparison of the Nyquist diagrams obtained from EIS measurements for bare and pBz-coated MS revealed that the coated samples exhibited a large, single capacitive loop, indicating enhanced corrosion resistance compared to bare MS. The existence of fluorine in amine was found to increase surface hydrophobicity, achieving a water contact angle of 146°, attributed to the fluorine groups' low van der Waals interaction with water, consistent with findings on the effects of fluorine in the study of Mydeen et al. [96]. Additionally, pBz synthesized with aee exhibited hydrophobicity (136°) due to the contribution of intermolecular hydrogen bonding. A comparison of the water contact angles of pBz coatings with curcumin and

fluorinated amines from this study, and those with curcumin but without fluorinated amines from the work of Muthukumar et al. [101] highlights the critical role of fluorine in enhancing hydrophobicity. The highest corrosion protection efficiency (99.84 % using Eq. (1)) was observed for the pBz with api due to the existence of imidazole core with nitrogen contributing to the corrosion protection [104]. Similarly, the study by Srinivasa et al. [97] reported nearly the same protection efficiency (99 % using Eq. (1)) for pBz coatings with api (ipa). Following the api coating, the next highest corrosion protection was achieved with adm, which provided 99.05 % efficiency related to its rigid nature with fused cyclohexane that can protect pBz structure from being corroded (Table 1).

Guaiacol derived from biomass hydrolysis with an aromatic structure in lignin molecules, is another compound that can be used for the formation of bio-based Bz resins [53,105,106]. L-tyrosine is an amino acid (rich in proteins), produced from green processes like the hydrolysis reaction of corn, casein, and other resources [107]. L-tyrosine can be used for the synthesis of Bz by having phenolic hydroxyl that contains aromatic amino acid [108]. Moreover, bio-based tyrosine-dipeptide can be obtained from L-tyrosine and be used in the synthesis of Bz (Fig. 6(a)) [54]. For this purpose, three different amines: aniline, dodecylamine, and furfurylamine, were used. It was observed that the improved cross-linked network of pBz with furfurylamine and aniline could increase flame retardant behavior. All the tyrosine-dipeptide-based samples showed hydrophobicity, however, the hydrophobic property was slightly higher for the pBz with dodecylamine. The reason for this observation is that this pBz enables the formation of a highly cross-linked network with a non-polar nature and inherent hydrocarbon moieties. The samples were used as coatings for MS (by spray coating), which showed proper corrosion resistance (with a corrosion inhibition efficiency of 98.3 % using Eq. (1) for the sample with furfurylamine) due to the existence of triazine cross-links that could reduce the anodic reactions [54]. The same as the study of Muthukumar et al. [101], the best corrosion protection performance was for the pBz coating with furfurylamine and the hydrophobicity was higher for the sample with a higher alkyl chain (dodecylamine). The comparison between these two studies also shows that the existence of curcumin in the Bz structure is effective in corrosion protection of MS substrates by comparing curcumin-furfurylamine- and tyrosine-furfurylamine-based pBz coatings corrosion inhibition efficiency.

Phenolic-rich Bzs were synthesized using lignin and phloretic acid, with stearylamine, furfurylamine, and ethanolamine serving as primary amine sources [109]. Due to its inherently hydrophobic nature, lignin contributed to the development of a hydrophobic coating when combined with stearylamine, achieving a water contact angle of 91°. This coating was noted for its ease of application. The hydrophobic properties of the resulting coating were comparable to those of lignin-based polyesters [110]. No corrosion evaluation techniques were employed in this study [109].

Cardanol has been used in the synthesis of bio-based Bz in the context of sustainable development [111]. Cardanol is obtained from cashew nut shells that can be used as the phenol source [112–114]. This compound with a long hydrocarbon chain (15 carbon atoms) has attracted attention in different applications like resins, surfactants, and coatings [115,116]. Cardanol was used as the phenol source along with stearylamine and paraformaldehyde for solventless Bz synthesis (Fig. 6(b)) [117]. Natural polyphenols can decrease the curing temperature of Bz. Moreover, adding a low amount of carboxylic acid to the Bz monomer can promote the curing of Bz [118]. Therefore, gallic acid as a polyphenol compound with a carboxyl group was used as the catalyst of ring-opening polymerization [117]. Cardanol is also used with silane-contained amine (3-aminopropyltriethoxysilane) as well as stearylamine for the synthesis of Bz monomer [119], which will be discussed in more detail in section 2.1.1.

To eliminate the release of antifouling agents that are usually used in conventional antifouling coatings and harm the marine ecosystem,

fouling-release coatings have been developed [120,121]. pBz coatings can be also used in antifouling coatings in marine applications by the release of fouling [122,123]. This phenomenon can happen by the release of fouling from the surface of coatings due to the low surface energy of the coating. Chen et al. [122] used cardanol and urushiol as phenol sources and it was observed that the existence of hydroxyl group excess in the phenolic group can reduce the activation energy and therefore, the curing temperature of the obtained Bz.

Another bio-based Bz monomer was synthesized using eugenol and three different amines (stearylamine, furfurylamine, and Dehydroabietylamine) by Zhang et al. [124]. Eugenol is an aromatic compound with an allyl group on its para position. Comparing electrochemical results showed the highest corrosion protection efficiency is for pBz coating obtained from eugenol and furfurylamine precursors with a value of about 89 % [124]. Furfurylamine along with pyrogallol can be used as the precursors for production of Bz monomers [125].

4-(Phenylazo)phenol, along with polyetheramine can be used for the synthesis of Bz monomer [126]. Polyetheramine is hydrophilic, and increasing the concentration of this compound in the Bz structure can decrease hydrophobicity. According to their study, the incorporation of flexible segments can improve the adhesion of Bz coatings to the substrate; moreover, the existence of lower flexible segments can increase the rigidity and the brittleness of the coatings. The obtained coating had impedance modulus in the order of  $10^4 \Omega \text{ cm}^2$  at low frequency (0.01 Hz) for coatings with a thickness of around 5  $\mu\text{m}$  and inhibition efficiency of 99 % (Eq. (1)) [126].

#### 2.1.1. Silane-functionalized pBz coatings

Silane groups can be employed in the functionalizing Bz coatings, thereby enhancing the adhesion between Bz resin and stainless steel through the formation of Fe–O–Si bonds [127]. Moreover, the use of silane in the coating allows the formation of a dual cross-linking network containing ring-opening polymerization of Bz and Si–O–Si bonds in the coating which enhances the barrier property and hydrophobicity of the coating and reduces water uptake. The chemical structure of 3-aminopropyltrimethoxysilane (3-APTMS) precursor is represented in Fig. 7 (a). Cross-linking points can be created by the reaction of active methoxy groups with moisture in the air, leading to increased cross-linking density. Therefore, functionalizing Bz with silane increases corrosion resistance [127]. A comparison between silane-functionalized pBz coatings and conventional pBz coatings revealed that the conventional pBz coating failed to provide uniform coverage, resulting in uncoated regions on the surface [127].

Silane-functionalized Bz can also be synthesized through the combination of silane-based and bio-based precursors such as cardanol, vanillin, eugenol, and guaiacol, enabling the production of bio-based Bz monomers [128]. Qu et al. [129] synthesized fluorinated silane-functional Bz to create a surface with a reduced free energy value of 15.5  $\text{mJ/m}^2$  which is desirable for lithographic applications.

Ye et al. [119] used cardanol with 3-aminopropyltriethoxysilane (silane-contained amine also called APTES) and stearylamine for the synthesis of Bz monomer. Both Bzs were used for coating MS substrates, and they showed hydrophobicity due to the long alkyl chains and the hydrogen bonds network. However, silane-functionalized Bz could create a dual-crosslinked network that contains polysiloxanes and pBz. Therefore, better corrosion protection could be observed for this coating at longer immersion times with an impedance modulus value of  $9 \times 10^6 \Omega \text{ cm}^2$  at 0.01 Hz after 60 days (obtained from EIS results), which is 10 times higher than the Bz monomer without silane functionality. This is due to the higher cross-linking density and barrier property that could prevent the penetration of corrosive ions.

Bz-based sol-gel coatings can also be produced to protect metallic substrates. Zhou et al. [130] synthesized Bz monomer with silane functionalities using APTES and p-cresol for further application in Bz-based sol-gel coating (Fig. 7(b)). For producing the sol-gel coating, Bz

Table 1

Summary of studies related to the pBz coatings with different molecular designs (the figures related to each study are mentioned for enhancing clarity).

Precursor/Monomer	Thickness ( $\mu\text{m}$ )	Substrate/Coating technique	Corrosive media	Notable corrosion protection properties	Reference
Bisphenol-A, aniline, and paraformaldehyde	2–5	MS Dip coating	3.5 wt% NaCl	The corrosion rate and corrosion current density were $5.07 \times 10^{-5}$ mm/year (Eq. (3)) and $4.36 \times 10^{-3}$ $\mu\text{A}/\text{cm}^2$ , respectively.	Lu et al. [41]
Pyrazolidine bisphenol, paraformaldehyde, dodecylamine (dda), octadecylamine (oda), and 4-fluoroaniline (Fig. 2(c))	20	MS Drop coating	3.5 wt% NaCl	The corrosion efficiency of the coating was 90 % (Eq. (1)) for the monomer with oda, showing the best corrosion protection.	Manoj et al. [85]
Bisphenol-F, 3-aminopropyltrimethoxysilane, and paraformaldehyde	5	MS and SS Spin coating	3.5 wt% NaCl	Obtaining coating with a corrosion rate of $3.68 \times 10^{-10}$ m/year (Eq.(2)) and a protection efficiency of 96 % (Eq. (1)) for pBz on MS.	Krishnan et al. [86]
1,4-phenylenediamine, phenol, and paraformaldehyde	2	Al alloy Spin coating	0.1 M NaCl	Impregnation of Bz with the surface of anodized Al alloy, making them suitable for further top coat application. Highly capacitive behaviour of pBz coating after one month of immersion.	Renaud et al. [88,144]
Phloretic Acid, 1,12- dodecandiol, ethylene glycol, polyethylene glycol, ethanolamine, paraformaldehyde	70	Al alloy Bar coating	0.1 M NaCl	The better corrosion protection of pBz coating while using dodecandiol after 50 days immersion in saline solution.	Van Renterghem et al. [3]
2-(4-Hydroxyphenyl)isoindoline-1,3-dione (pPP), 2-(2-Hydroxyphenyl)isoindoline-1,3-dione (oPP), p-toluidine, and paraformaldehyde (Fig. 3(a), (b))	5	MS Spin coating	3.5 wt% NaCl	The better corrosion protection while curing Bz at 180 °C in the case of both monomers. The higher protection efficiency for pPP coating (98 % obtained by Eq. (1)), due to the better adsorption of this monomer to the MS substrate.	Aly et al. [45, 145]
n-propyl-3,4-dihydro-6-methyl-2H-1,3-benzoxazine, and n-propyl-3,4-dihydro-6-phenoxy-2H-1,3-benzoxazine (POP-b) (Fig. 3(c), (d))	7.8–9.4	Al alloy Dip coating	3.5 wt% NaCl	A decrease in adhesion by application of pBz along with Bz-based sol-gel due to the creation of a higher thickness coating than the sol-gel alone. Increased corrosion protection by having two-layer coatings. Better corrosion protection of POP-b coating.	Li et al. [93]
Thymol, methylamine, ethylamine, propylamine, butylamine, and paraformaldehyde (Fig. 4)	–	SS304 Spin coating	1 M NaCl	Decrease in corrosion rate by increasing curing temperature. The lowest corrosion rate for Bz with longer alkyl chain amine (butylamine) with an anticorrosion efficiency of 99 % (Eq. (1)).	Suesuwan et al. [49]
Furfural bis-thymol, fluorine substituted amines (fluoroaniline, trifluoromethylaniline (tfma), 4-fluoro-3-trifluoromethylaniline (fma), pentafluoroaniline (pfa), pentafluorosulphanylaniline (pfsa)), and paraformaldehyde	–	MS Spray coating	–	Increasing the corrosion protection of the coating with increasing the fluorine content in the primary amine. Corrosion protection efficiency of 99.99 % for coating with pfsa, obtained from Eq. (1).	Mydeen et al.
TTM, ipa, dmapa, aee, and paraformaldehyde (Fig. 5 (a))	2000	MS Spray coating	3.5 wt% NaCl	The inhibition efficiency of 99.9 % (Eq. (1)) for the pBz coating obtained from dmapa.	Srinivasan et al. [97]
SF-BZ 2OH, p-toluidine, and paraformaldehyde (Fig. 5 (b))	2	MS Dip coating	3.5 wt% NaCl	The inhibition efficiency and the corrosion rate value of 92 % (Eq. (1)) and 22 $\mu\text{m}/\text{year}$ (Eq. (2)), respectively, for the coating with 300 g/L Bz concentration.	Mahdy et al. [44,146]
Salicylaldehyde, n-hexylamine, formaldehyde	4	MS Spray coating	0.1 M $\text{H}_2\text{SO}_4$	Production of Schiff base pBz coating, effective in the corrosion protection of substrate in acidic media.	Soliman et al. [43]
hydroxynaphthaldehyde and AG, BG, and MA (to form phenolic precursors), furfurylamine, paraformaldehyde	–	MS Spray coating	3.5 wt% NaCl	Achieving coatings with hydrophobic properties and corrosion protection efficiencies around 140° and 99 %, respectively.	Krishnan et al. [100]
Curcumin, aniline, furfurylamine, octadecylamine, paraformaldehyde	–	MS Drop coating	3.5 wt% NaCl	The water contact angle of 137° for pBz with octadecylamine. The corrosion inhibition efficiency value of 99.6 % (Eq. (1)) for the pBz coating with furfurylamine.	Muthukumar et al. [101]
Curcumin, adamantylamine (adm), aniline (a), allyl amine (aa), amino ethoxyethanol (aee), amino propyl imidazole (api) and trifluoro methyl aniline (tfma),	11.95–17.22	MS Spray coating	3.5 wt% NaCl	The highest water contact angle for pBz with tfma and a value of 146°. The highest inhibition efficiency for the pBz coating with api with a value of 99.84 % (Eq. (1)).	Madesh et al. [104]
L-tyrosine cyclic dipeptide, aniline, dodecylamine, furfurylamine, and formaldehyde	–	MS Spray coating	3.5 wt% NaCl	The best corrosion protection for the coating with furfurylamine and corrosion protection efficiency of 98.3 %.	Mohamed Mydeen et al. [54]
Polyetheramine, 4-(phenylazo)phenol, paraformaldehyde	5	Low-carbon steel Drop coating	3.5 wt% NaCl	Overcoming traditional brittle pBz coating with the help of polyetheramine and improving corrosion protection by creating the barrier layer between corrosive media and the substrate.	Zhao et al. [126]
Paraformaldehyde, 3-APTOS, bisphenol-A (Fig. 7(a))	5	MS and SS Dip coating	3.5 wt% NaCl	Decrease in the corrosion current while using the synthesized pBz. Obtaining the corrosion current density of $0.59 \pm 0.08$ $\mu\text{A cm}^{-2}$ for pBz-coated MS samples and $1.55 \pm 0.35$ $\text{nA cm}^{-2}$ for pBz coated SS.	Zhou et al. [127]

(continued on next page)

Table 1 (continued)

Precursor/Monomer	Thickness ( $\mu\text{m}$ )	Substrate/Coating technique	Corrosive media	Notable corrosion protection properties	Reference
Cardanol, APTES, stearylamine, and paraformaldehyde	26	MS Automatic coating machine	3.5 wt% NaCl	The charge transfer resistance value of $3.12 \times 10^7 \Omega \text{ cm}^2$ after two months for the silane-based coating.	Ye et al. [119]
APTES, p-cresol, and paraformaldehyde (Fig. 7(b))	$0.5 \pm 0.1$	Al alloy Dip coating	3.5 wt% NaCl	The higher corrosion resistance performance for the TEOS-pBz coating that was cured at $210^\circ\text{C}$ . The highest impedance modulus at low frequency for the homopolymerized coating with the value of $10^5 \Omega \text{ cm}^2$ after 30 days of immersion.	Zhou et al. [130, 147]
Eugenol, dehydroabietylamine, and paraformaldehyde. 6-allyl-8-methoxy-3-octadecyl-3, 4-dihydro-2H-benzoxazin. 6-allyl-3-(furan-2-ylmethyl)-8-methoxy-3, 4-dihydro-2H-benzoxazine	–	Q235 carbon steel	3.5 wt% NaCl	Using different concentrations of monomers to produce copolymers with the least corrosion rate $1.4 \times 10^{-5} \text{ mm/year}$ .	Zhang et al. [124,148,149]
Furfurylamine, pyrogallol, eugenol, stearylamine, paraformaldehyde	27	MS automatic film coater	3.5 wt% NaCl	Production of hydrophobic coating with a water contact angle of $110^\circ$ after copolymerization. Corrosion inhibition of coatings after 30 days immersion.	Chen et al. [125]
Cardanol, N,N'-Bis(2-aminoethyl)ethane-1,2-diamine, and paraformaldehyde	–	MS Flow coating method	3.5 wt% NaCl	Mixing Bz monomers with epoxy for further curing, causing an increase in the corrosion resistance efficiency to 99.9 % (Eq. (1))	Patil et al. [137]
3-APTMS, bisphenol-A, paraformaldehyde	5	MS Dip coating	3.5 wt% NaCl	Corrosion protection efficiency of 99 % (Eq (1)), after copolymerizing epoxy with 30 % Bz-TMOS.	Zhou et al. [138]
Guaiacol, paraformaldehyde, and ethanolamine	–	MS Flow coating method	3.5 wt% NaCl	Mixing monomer with isocyanate (as hardener) in different concentrations and a protection efficiency of 99.9 % (Eq. (1)).	Phalak et al. [105]

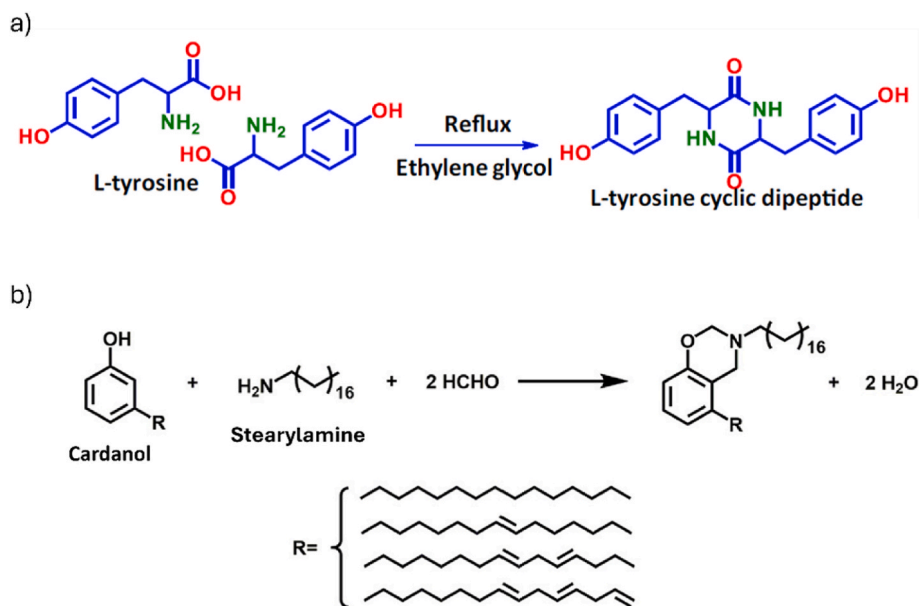


Fig. 6. a) Synthesis of L-tyrosine cyclic dipeptide used for production of Bz monomer, reproduced with permission from Ref. [54], b) preparation of Bz monomer with cardanol and stearylamine, reproduced with permission from Ref. [117].

monomer was mixed with tetraethoxysilane (TEOS) and applied on Al alloy. In their study, they claimed that higher curing degree and higher cross-linking density, as well as hydrophobicity are key factors causing better corrosion protection [130]. The incorporation of Bz could enhance the cross-linking density and hydrophobicity of the sol-gel coatings [131]. In the study of Zhou et al. [131], the performance of Bz-based sol-gel coatings was evaluated by incorporating varying amounts of Bz monomers into the sol-gel solution with TEOS. The results indicated that increasing Bz monomer content in the sol-gel preparing solution increased corrosion resistance of the resulting coating, with the highest impedance modulus of  $10^5 \Omega \text{ cm}^2$  at 0.01 Hz (from Bode diagrams and EIS results) achieved using a homopolymerized pBz coating

after 30 days of immersion in a saline solution. The addition of Bz monomer produced dense coatings with hydrophobic surfaces, contributing to improved stability and prolonged substrate protection during extended immersion times. Fig. 8 illustrates the increased hydrophobicity of the coatings with higher Bz monomer content.

### 2.1.2. Bz-based organic coatings (mixture of Bz and other monomers)

The barrier properties of coatings, and subsequently their corrosion protection, can be enhanced through the augmentation of the cross-linking density of the coating [122,132]. The cross-linking density can be enhanced by increasing the number of cross-linking Bz rings [133], as well as increasing the number of cross-linking points through the

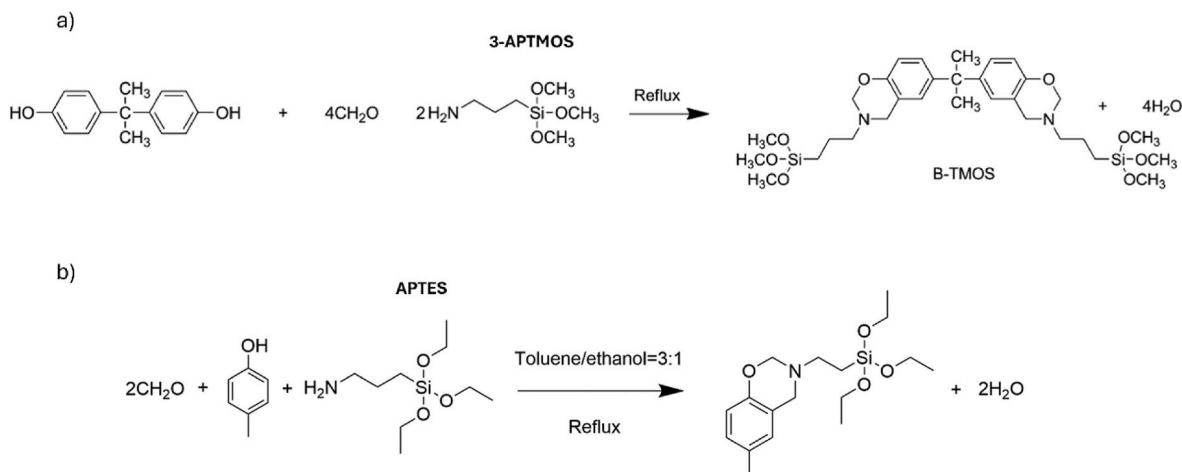


Fig. 7. Synthesis of silane-functionalized Bz monomer with a) 3-APTOS and b) APTES, reproduced with permission from Ref. [127] and Ref. [130], respectively.

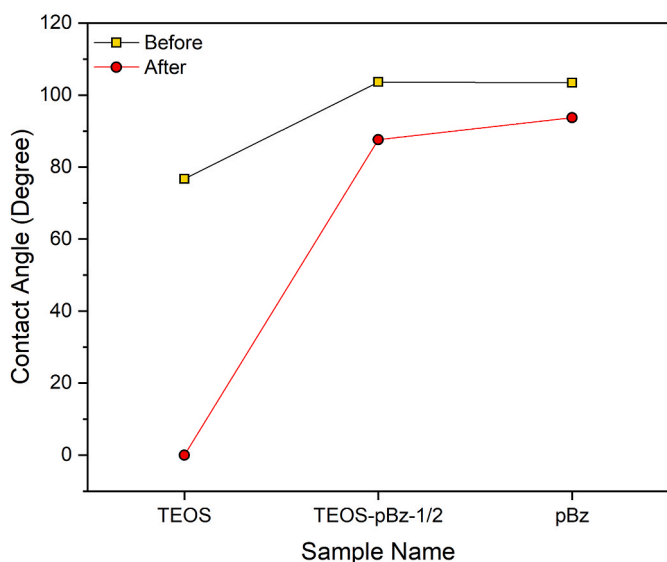


Fig. 8. Increased water contact angles with the addition of Bz to the sol-gel coatings before and after one month of immersion in saline solution, reproduced based on Ref. [131].

incorporation of compounds like epoxy [134–136]. Different Bz monomers can be polymerized together for better corrosion protection properties. Zhang et al. [124] copolymerized eugenol-based Bz monomer with different amines. Copolymerizing Bz monomers increases the corrosion protection of pBz coatings by increasing both the cross-linking density and hydrophobicity. The corrosion protection efficiency of these pBz coatings increased to more than 99 % (Eq. (1)) by copolymerizing Bz monomers compared to approximately 89 % (Eq. (1)) for homopolymerized pBz coatings (as observed with Bz monomers containing furfurylamine). Copolymerization of eugenol-based Bz monomer with pyrogallol-based Bz monomer reduced the curing temperature and increased cross-linking density due to the presence of furfuryl moieties and phenolic hydrogens. This improvement enhanced corrosion protection nearly eightfold compared to a bare MS substrate, as evidenced by the impedance modulus at 0.01 Hz, reaching around  $10^{11} \Omega \text{ cm}^2$  (from EIS measurements) for copolymerized coatings. Additionally, the water contact angle of the copolymerized coatings increased from  $92^\circ$  to  $110^\circ$ , indicating higher hydrophobicity, which further contributes to improved corrosion resistance [125].

Patil et al. [137] synthesized Bz with cardanol and an amine with

multiple nitrogen atoms for anti-corrosion application. They also copolymerized Bz with epoxy, which had better chemical and mechanical properties than pBz coating due to the creation of a dual cross-linked network caused by copolymerization with epoxy. Moreover, better corrosion protection performance of copolymerized Bz was observed using electrochemical analysis. The corrosion current obtained from pBz alone and the best copolymerized pBz with epoxy (epoxy equivalent weight of 500 gm/mol) was  $4.3 \mu\text{A}$  and  $0.01 \mu\text{A}$  (obtained from the Tafel curves), respectively, representing the effectiveness of copolymerizing pBz with epoxy which was further confirmed with salt spray results.

Bz-TMOS was also used as a curing agent for the epoxy coating to increase the hydrophobicity and, consequently, the corrosion resistance of the coating [138]. With the existence of intermolecular hydrogen bonds in pBz coatings, the cross-linking cannot be completed. Since these intermolecular hydrogen bonds reduce the fluidity and availability of functional groups to participate in the cross-linking reactions [139]. For this reason, epoxy can be used in the polymerization of pBz to form a stable covalent (and reduce hydrogen bond formation) with phenolic hydroxyl group in Bz to promote the crosslinking density [34]. In the study of Zhou et al. [138], the dual cross-linking and hydrogen-bonding network within the pBz-TMOS matrix includes covalent cross-links and hydrogen bonding between the pBz and epoxy components. Phenolic OH groups from the ring-opening reaction of Bz can react with epoxide (in epoxy), resulting in the enhancement of mechanical properties and hydrophobicity (decrease in surface energy), consequently improving corrosion resistance. The possible reactions are shown in Fig. 9. The corrosion protection efficiency increased from 96.7 % in epoxy coating to 99.5 % for epoxy cured with 30 % Bz-TMOS coating.

Isocyanate can be used as a hardener for the curing process of Bz monomer. In the study of Phalak et al. [105] a guaiacol-based Bz monomer was obtained and then it was cured with isocyanate. Increasing urethane in the pBz structure could improve corrosion protection. Comparing the obtained corrosion protection results with the neat pBz coatings revealed enhanced corrosion protection with efficiency of 99 % (Eq. (1)), which is due to the increased cross-linking density that can prevent diffusion of corrosive ions [105]. An eugenol-based Bz resin was also cured with polyurethane and applied as a coating for the corrosion protection of MS [140]. Similar behavior was observed, wherein increased polyurethane content resulted in improved corrosion protection. In this case, the corrosion protection efficiency reached approximately 98 % (Eq. (1)) [140].

Chen et al. [141] synthesized urushiol-based Bz catalyzed by copper chloride which resulted in the production of urushiol-based Bz copper polymer. The chemical structure of urushiol is presented in Fig. 10(a). This polymer was then used with polymerized tung oil for antifouling coating application [123]. It was observed that the long alkyl chain of

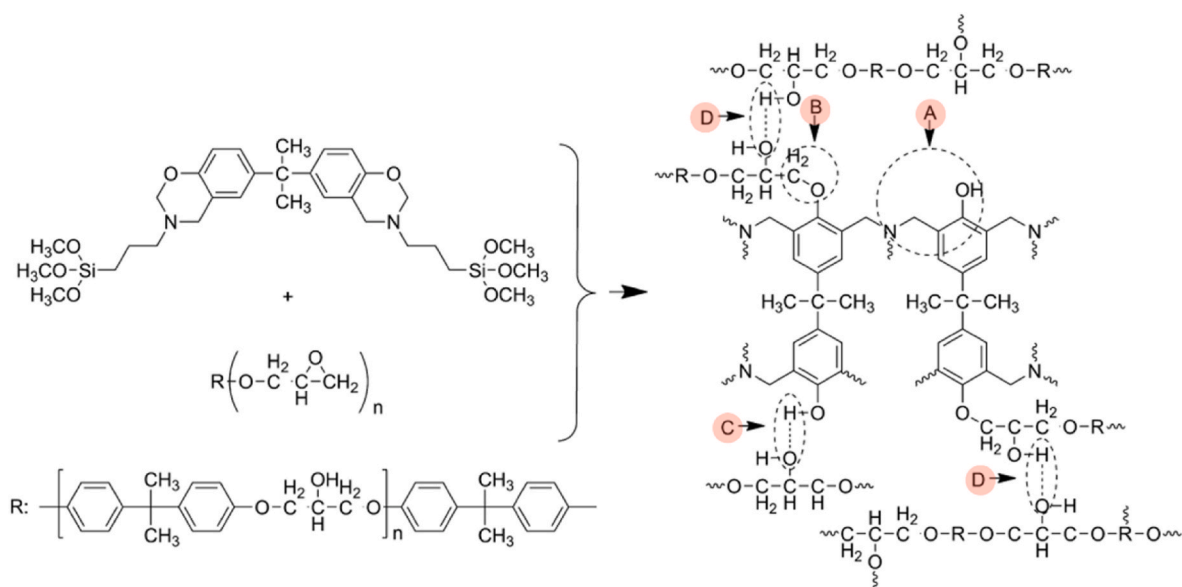


Fig. 9. Copolymerization process, (A) ring-opening of oxazine ring, (B) etherification reaction, (C) epoxy and pBz hydrogen bonding interactions, (D) the stretching vibrations related to the self-associated hydroxyl groups, reproduced with permission from Ref. [138].

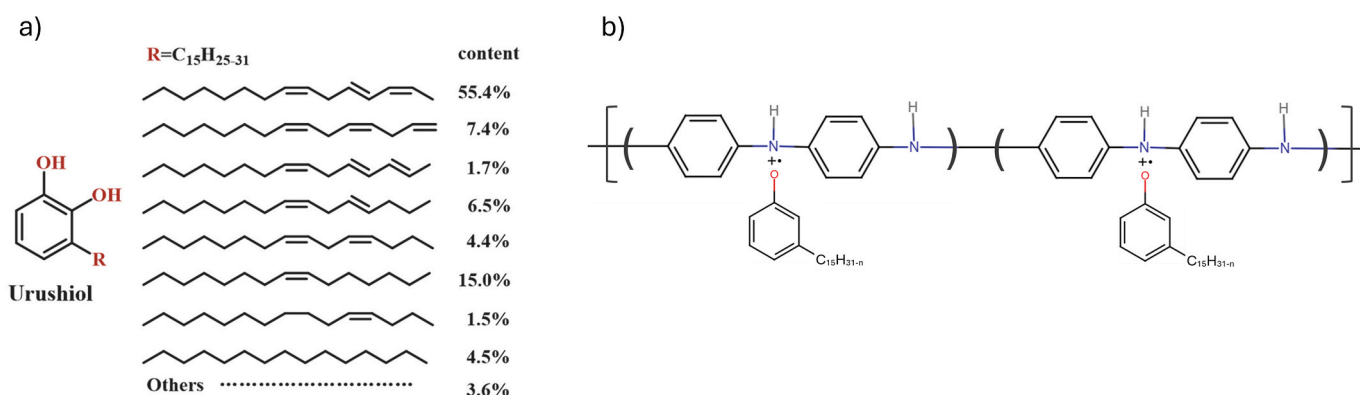


Fig. 10. Chemical structure of a) urushiol, reproduced with permission, based on Ref. [141] and b) cardanol-doped polyaniline, reproduced based on Ref. [143].

tung oil as well as copper ions were effective in the antifouling property of the coating. In another study by this group, they incorporated silver nanoparticles in the coating to enhance the antifouling properties [142].

Cardanol-doped polyaniline as the curing agent (Fig. 10(b)) with Bz prepolymer was also used for coating application [143]. This coating could enhance corrosion protection by improving the cross-linking density. Moreover, the addition of cardanol-doped polyaniline could decrease the curing temperature by adding another ring-opening reaction mechanism. The existence of cardanol in the polyaniline structure enhanced the homogenous dispersion of polyaniline in pBz as well as the adhesion of the coatings to the substrates (the adhesion strength with and without cardanol-doped polyaniline was around 0.5 MPa and 0.3 MPa, respectively for the coatings with a thickness of around 250  $\mu\text{m}$ ), resulting in better corrosion protection performance. The enhanced adhesion can be attributed to the nitrogen groups and  $\pi$ -conjugated systems in polyaniline, which provide electrons that increase interactions with the metallic substrate. Additionally, the presence of cardanol introduces hydroxyl groups, further contributing to improved adhesion [143].

Table 1 shows the summary of the studies related to the corrosion protection of Bz coatings with different chemical structures.

## 2.2. PBz coatings with additives

Blending polymers with different additives can not only enhance the thermal and mechanical properties of the composites [150] but also improve the corrosion protection of the resulting organic coatings [151].

### 2.2.1. PBz coatings with nanoparticles/nanoplatelets

Incorporating nanoparticles into the coatings can enhance the organic coating's corrosion resistance, mechanical strength, and thermal properties. For instance, Hexagonal boron nitride was used to make a composite coating that can enhance the corrosion protection of coatings by adding hydrophobicity [152–154]. Boron nitride is a 2-dimensional material with a layered structure in which boron and nitride are bonded covalently and are combined through van der Waals forces [152, 155]. They have good thermal stability, electrical insulation, and chemical resistance [156,157]. Wang et al. [153] added hexagonal boron nitride to the bio-based Bz to provide a superhydrophobic coating. The addition of hexagonal boron nitride to the cardanol and stearylamine-based Bz has been shown to improve corrosion resistance, mechanical strength, and thermal properties of the pBz coating [117]. The mechanism for the corrosion protection of the resulting coating is illustrated in Fig. 11(a). Hexagonal boron nitride as well as the superhydrophobic surface of the coating prevent the penetration of corrosive

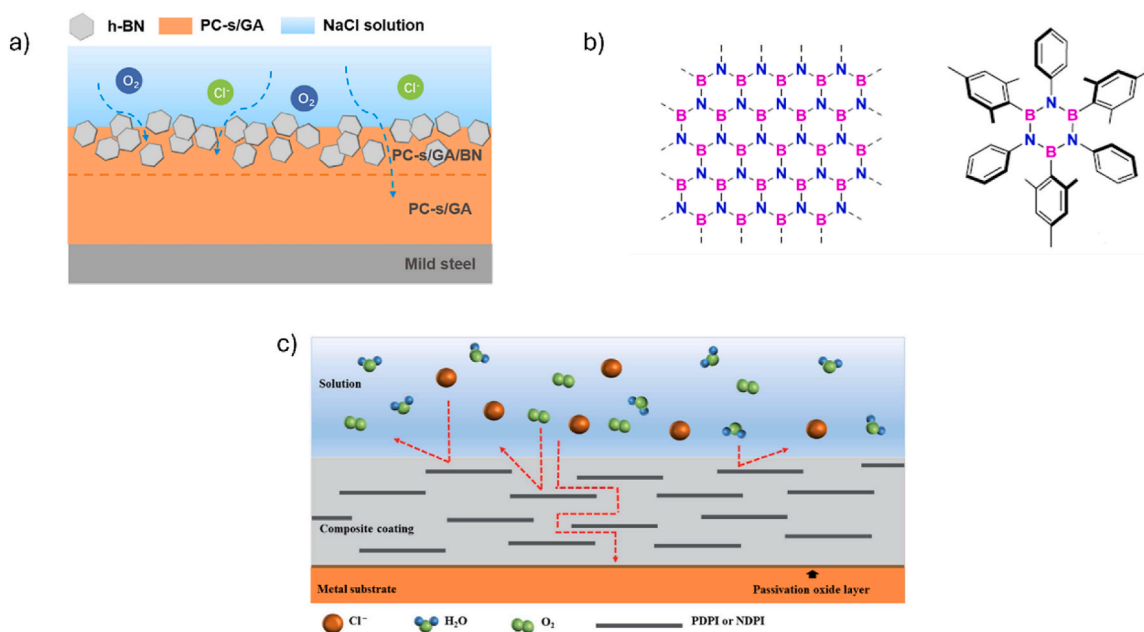


**Fig. 11.** a) The obtained coating with pBz (PC-s/GA that is obtained from cardanol and stearylamine (PC-s), and cured with gallic acid (GA)) and hexagonal boron nitride (h-BN), reproduced with permission from Ref. [117]. b) h-BN 2D structure and the chemical structure of borazine derivative, reproduced with permission from Ref. [158]. c) The corrosion protection mechanism of the composite coating, reproduced from Ref. [48] with permission from the Royal Society of Chemistry.

ions and, thereby enhancing corrosion protection. Renaud et al. [158] used B-trimesityl-N-triphenylborazine (borazine derivatives in Fig. 11 (b)) with Phenol-paraPhenyleneDiAmine and observed improved corrosion protection of Al alloy by increasing the hydrophobicity of the coating (increased water contact angle from 72.5° to 97° due to the hydrophobic nature of borazine). The impedance modulus at low frequency (0.01 Hz) remained almost constant in the order of  $10^9 \Omega \text{ cm}^2$  after one-month of immersion for pBz coating containing 0.5 wt% borazine. Moreover, borazine could be homogeneously dispersed throughout the coating. Zhou et al. [159] added SiO<sub>2</sub> nanoparticles in silane-functionalized Bz (pBz-TMOS) and a hydrophobic coating with barrier properties and increased corrosion resistance was obtained. The enhanced properties were due to the reaction of silanols in pBz-TMOS (hydrolysis of the alkoxy groups) with the hydroxyl groups on the surface of SiO<sub>2</sub> nanoparticles through covalent bonding, resulting in a strong interaction between the two phases. SiO<sub>2</sub> nanoparticles could reduce the corrosion rate 15 times at the optimum concentration of 5 wt % [159].

Salicylaldehyde azine-functionalized Bz with the addition of nanoclays as well as epoxidized soybean was used as the coating for corrosion protection of MS [34]. The adhesion of the monomer to the substrate was enhanced compared to its polymerized form. Additionally, the addition of epoxy improves adhesion and facilitates the formation of stable chemical bonds with pBz, thereby creating dense crosslinking. The incorporation of nanoclay in the coating effectively reduces coating porosity and alters its diffusion pathway. As a result, the coating exhibits proper corrosion resistance with corrosion protection efficiency of 99.63 % in acidic environments [34].

As mentioned, Bz resins have certain limitations, including a high curing temperature (>200 °C) that prevents them from being used on heat-sensitive metals like magnesium. Chen et al. [48] produced cardanol-based Bz and used CuCl<sub>2</sub> as the catalyzer of the ring-opening reaction to make curing at room temperature possible. Moreover, they used two-dimensional lamellar structure polyimides (pyromellitic dianhydride polyimide (PDPI) and 1,4,5,8-naphthalene tetracarboxylic dianhydride polyimide (NDPI)) with a two-dimensional sheet structure act as corrosion inhibitors because of changes in electrolyte pathways to the substrate and delay the corrosion process (Fig. 11(c)). Besides, lone

pairs of electrons in nitrogen atoms create coordination bonds with metal cations and form a protective layer on the substrate. With this approach, an eco-friendly, bio-based, and low-cost coating was obtained [48].

pBz itself can be used as an additive to varnish to increase corrosion protection. Malathi Devi et al. [160] used activated carbon obtained from disposed plastics with pBz to form a composite coating. Activated carbon is an additive for organic coatings which can be obtained from waste materials at a low cost [161–164]. To prepare the coatings, the carbon and pBz composite was converted to a fine powder, and then the powder was mixed with a commercial varnish. The coatings were applied on the mild steel substrates by brush manually [160]. Comparative analysis of the corrosion protection by the coatings reveals that the incorporation of pBz and carbon/pBz into the varnish enhances the protection efficiency from 85 % to 97 % and 99.5 %, respectively. This improvement can be attributed to increased hydrophobicity, stemming from the hydrophobic nature of pBz, enhanced adhesion due to the presence of hydroxyl groups in pBz, and the inclusion of composite powders, which further enhance corrosion resistance by altering the pathways for electrolyte diffusion [160].

### 2.2.2. PBz coatings with corrosion inhibitors

The addition of corrosion inhibitors directly to the matrix of organic coating can affect the mechanical properties due to the lack of compatibility between organic coating and corrosion inhibitors [72, 165]. Moreover, for long-term corrosion protection, a controlled release of corrosion inhibitor is needed rather than constantly releasing it. For this purpose, corrosion inhibitors should be preserved in an appropriate container that is compatible with the corrosion inhibitor, coating, and substrate [73,166].

In the study of Xu et al. [165] benzotriazole in halloysite nanotubes was added to the pBz coating as a corrosion inhibitor for the protection of carbon steel. These nanocontainers release corrosion inhibitors in response to pH variations during corrosion reactions, with an increase in pH near cathodic regions due to the reduction of oxidants and a decrease in pH near anodic regions as a result of corrosion product hydrolysis. This targeted release mechanism operates in proximity to cathodic and anodic areas. It was shown that the release and adsorption of

benzotriazole can create a protective layer to further prevent corrosion [165]. It was observed that the optimum weight percentage of nanocontainers with benzotriazole to enhance corrosion resistance is 3 wt%, increasing the impedance modulus at 0.01 Hz to a value of  $1.48 \times 10^9 \Omega \text{ cm}^2$  which is two orders of magnitude compared to the neat pBz coating. Fig. 12(a) illustrates the corrosion inhibition mechanism for this coating.

### 2.2.3. PBz coatings with corrosion inhibitors and nanoparticles/nanoplatelets

Corrosion inhibitors as well as nanoparticles can be used at the same time in double-layer coating to create an active coating along with hydrophobic coating. Cao et al. [167] used pBz coating with 2-mercaptobenzimidazole incorporated in halloysite nanocontainers as a primer and made a superhydrophobic topcoat by adding  $\text{SiO}_2\text{-NH}_2$  nanoparticles. Fig. 12(b) shows the structure of the coating. The uniform distribution of nanoparticles generates micro- and nano-scale roughness on the surface of the coating. Additionally, Bz resin exhibits low surface energy, which contributes to the formation of a superhydrophobic coating. Consequently, this combination, along with the controlled release of corrosion inhibitors at corroded sites and the formation of a protective layer (reacting inhibitor with Fe cations and their adsorption on the substrate), enhances the corrosion resistance performance of the double-layer coating on a carbon steel substrate six orders higher than the plain pBz coating. Moreover, the presence of nanoparticles and nanocontainers in the coatings modifies the pathways for electrolyte diffusion, creating a more tortuous route that hinders the electrolyte from reaching the substrate, thereby mitigating further corrosion [167].

### 3. Bz as corrosion inhibitors

Bz can inhibit corrosion due to the oxazine heterocycle (connected to the benzene ring) in which heteroatoms with electron pairs exist [70, 71]. In this regard, Kadhim et al. [69] used 2-Methyl-4H-benzo[d][1,3]oxazin-4-one (BZ1) and 3-amino-2-methylquinazolin-4(3H)-one (BZ2) as corrosion inhibitor for corrosion protection of MS in acidic medium. They investigated the effect of the amino group in the inhibitor, the concentration of the inhibitor in an acidic solution, and the temperature of the corrosive medium on the corrosion of the substrate. The inhibition efficiency was increased with increasing the concentration of inhibitor and decreasing the temperature. The decrease in inhibition efficiency with increasing temperature can be attributed to the increased mobility of inhibitors, resulting in a decrease in the interaction between molecules and the surface, as well as the desorption of adsorbed inhibitor molecules [168,169]. The donation of non-bonding electron pairs in nitrogen or oxygen in inhibitor to the Fe cations from the substrate results in the formation of complexes that establish a protective layer on the surface. Fig. 13(a) shows the inhibition mechanism of these

inhibitors. Fig. 13(b) represents the SEM images of samples with and without corrosion inhibitors, highlighting the potential formation of a protective layer and a smoother surface in the case of inhibitor. In contrast, the surface is highly damaged and corroded without the inhibitor in the acidic solution.

A higher inhibition efficiency was observed for BZ2 (more amino groups), with an inhibition efficiency of 89 % at 30 °C, due to its higher tendency for electron donation. The amino group of the inhibitor changes the electronic property (electronegativity) of organic molecules. In general, the lower electronegativity of organic molecules leads to higher electron donation and higher inhibition [69]. In another study, Ugin Inbaraj et al. [71] produced corrosion inhibitor from paracetamol, benzylamine, and formaldehyde precursors to form 6-acetamido-3-benzyl-3,4-dihydro-2H-1,3-benzoxazine (ABB). It was shown that this inhibitor can be absorbed on the surface by chemisorption due to the negative charge of oxygen and nitrogen lone pair electrons as well as aromatic rings'  $\pi$  electrons (obtained from theoretical calculations). Moreover, physisorption can take place by the electrostatic attraction of the aromatic ring. For further investigation, surface analysis was conducted using AFM and SEM imaging. The results revealed a smoother surface and reduced corrosion on substrates immersed in the acidic solution containing the inhibitor [71]. They also investigated the effect of temperature and inhibitor concentration on corrosion inhibition, observing trends consistent with the findings of Kadhim et al. [69], where corrosion inhibition efficiency increased with higher inhibitor concentrations and decreased with rising temperature. At the optimum concentration, the inhibition efficiency of BZ2 on MS at 40 °C was reported as 79 % [69]. Similarly, at the optimum concentration, ABB demonstrated inhibition efficiencies of 98 % on high carbon steel and 93 % on Al [71] (Table 3). The corrosion inhibition efficiency of ABB was evaluated using potentiodynamic polarization measurements. In general, corrosion inhibitors influence anodic and/or cathodic reactions [170]. In the case of ABB, changes in both cathodic and anodic slopes were observed, indicating a mixed-type corrosion inhibitor. However, the more significant change in the cathodic slope suggests that the inhibitor is predominantly cathodic control.

Alamry et al. [70] added electron-rich atoms oxygen and nitrogen as well as sulfur, to investigate the effect of functional groups on corrosion inhibition of Bz corrosion inhibitor. EIS, potentiodynamic polarization, and linear polarization resistance were used for this purpose. It was observed that the corrosion inhibition could take place using chemisorption and physisorption [70]. They confirmed that physisorption can happen by the interaction of protonated species of the corrosion inhibitor with the  $\text{Cl}^-$  that is previously absorbed on the steel substrate. In addition, chemisorption takes place by the donation of lone electron pairs of the corrosion inhibitor to the empty orbital of Fe from the substrate. There's also another adsorption mechanism that is called

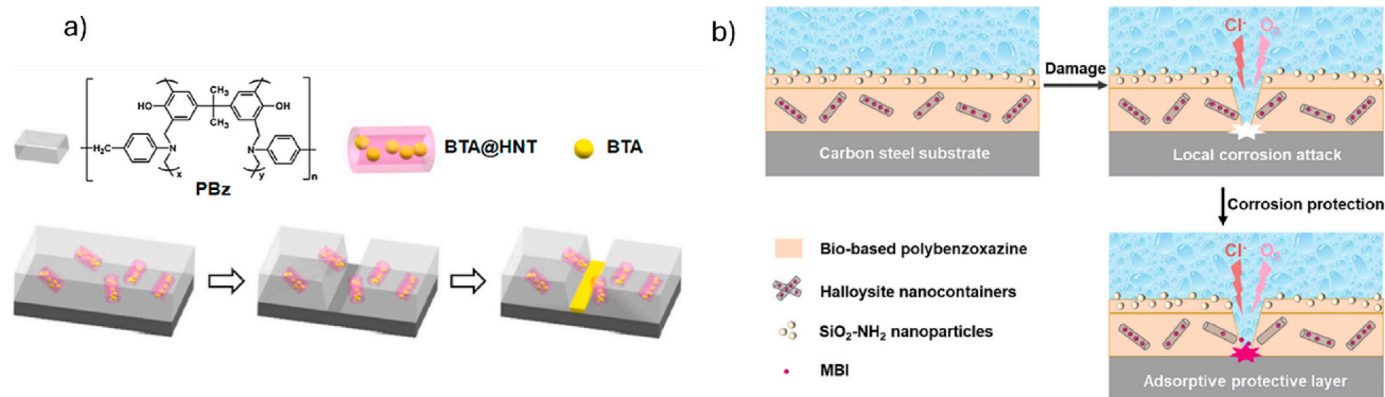
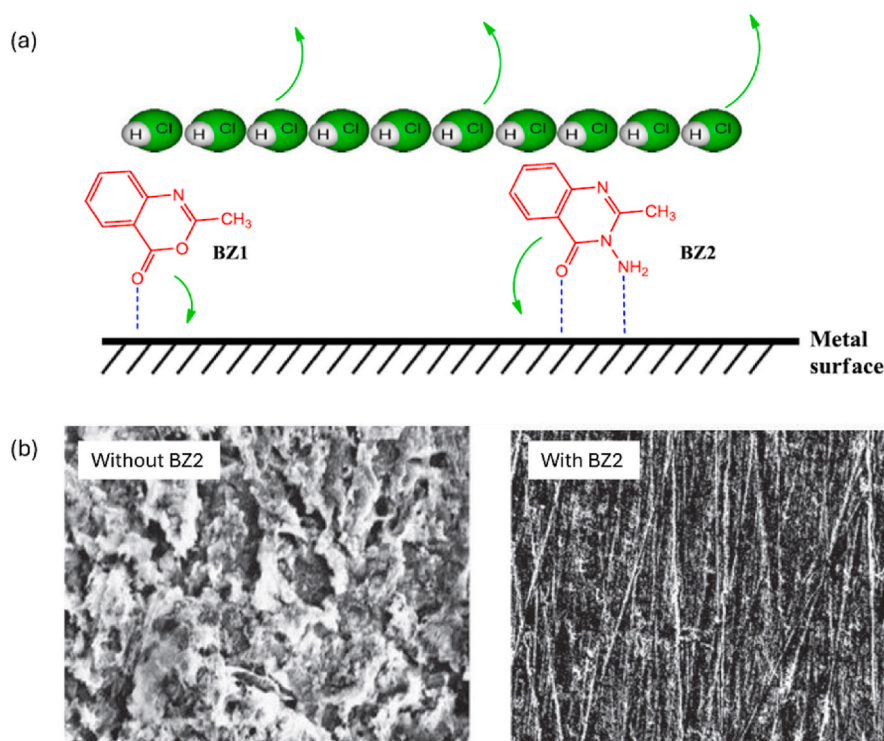


Fig. 12. a) Self-healing performance of pBz coating containing benzotriazole (BTA)-loaded halloysite nanotubes (HNT), reproduced with permission from Ref. [165]. b) Mechanism of corrosion protection with 2-mercaptobenzimidazole (MBI), reproduced with permission from Ref. [167].



**Fig. 13.** a) Inhibition mechanism of BZ1 and BZ2, and b) SEM images of the surface of MS with and without BZ2 in acidic solution at 30 °C, reproduced with permission, based on Ref. [69].

retro-donation, in which the accumulated negative charges on the substrate can be moved to the unoccupied  $\pi$  anti-bonding of the corrosion inhibitor [70,171]. Fig. 14 illustrates these adsorption mechanisms on the carbon steel substrate.

In addition to investigating the corrosion inhibition mechanism of the Bz molecule, the study examined the effects of Bz concentration and temperature on inhibition efficiency. As noted earlier, increasing the inhibitor concentration enhances inhibition efficiency. In this study, an efficiency of 88 % was achieved at room temperature with an inhibitor concentration of 600 ppm. Generally, the corrosion rate of metals increases with rising temperature due to the elevated kinetic energy of the corrosive medium [172]. In this study, the corrosion rate increased slightly with temperature, rising from 0.448 mm/year at room temperature to 0.974 mm/year at 40 °C and 4.56 mm/year at 60 °C (at the optimum concentration of 600 ppm). Notably, the corrosion rate at

60 °C in this study is significantly lower than the accepted corrosion rate of 50.80 mm/year in acidic environments [173].

The Langmuir adsorption isotherm model is used for fitting data and calculating the Gibbs free energy of adsorption ( $\Delta G_{ads}^\circ$ ) [70]. Generally, the type of adsorption is determined by calculating the Gibbs free energy of adsorption and verifying its range according to Table 2 [70]. The  $\Delta G_{ads}^\circ$  value of  $-25$  kJ/mol, confirms the existence of both chemisorption and physisorption.

Chemisorption involves charge sharing and electron transfer from the inhibitor to the substrate surface, resulting in interactions stronger than the van der Waals forces in physisorption. At 600 ppm concentration of inhibitor, the inhibition efficiency slightly increased from 88 % at room temperature to 90 % and 91 % at 40 °C and 60 °C, respectively, suggesting a predominant chemisorption mechanism (Table 3).

The SEM images of the carbon steel surface immersed in HCl solution, with and without the inhibitor, are presented in Fig. 15(a),(c). The images reveal that the surface of the samples with the inhibitor is smoother and free of cracks. Additionally, EDS analysis (Fig. 15(b),(d)) of the chemical composition of the formed film on the surface indicated a higher concentration of Fe and a reduced presence of Cl and oxygen when the inhibitor was used, correlating with decreased corrosion. Furthermore, the appearance of peaks corresponding to N and S elements in the sample with the inhibitor provides further evidence of the inhibitor's adsorption onto the surface.

All studies demonstrated the effectiveness of Bz as a corrosion inhibitor, highlighting its high inhibition efficiency in acidic environments and at temperatures exceeding room temperature. The inhibition efficiencies of Bz corrosion inhibitors were observed to be more than 80 %

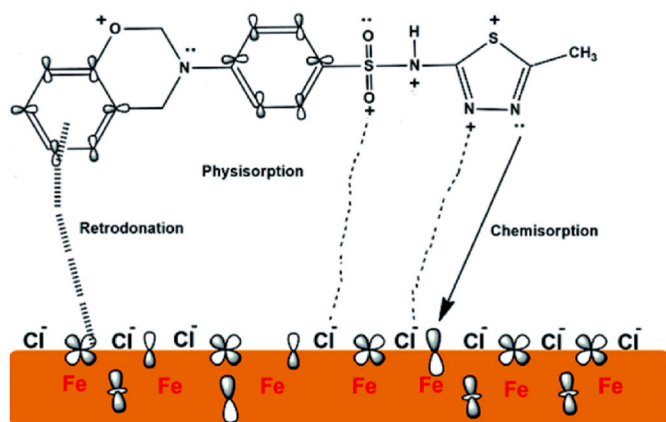


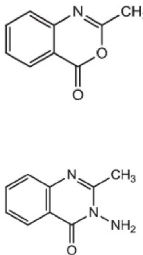
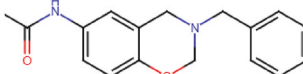
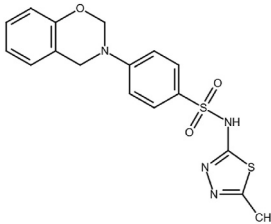
**Fig. 14.** Different adsorption mechanisms for the organic corrosion inhibitor on carbon steel substrate, reproduced from Ref. [70] with permission from the Royal Society of Chemistry.

**Table 2**

The relation between Gibbs free energy of adsorption and the adsorption mechanism.

$\Delta G_{ads}^\circ$ around $-20$ kJ/mol	Physisorption
$-40$ kJ/mol $\leq \Delta G_{ads}^\circ$	Chemisorption
$-40$ kJ/mol $\leq \Delta G_{ads}^\circ \leq -20$ kJ/mol	Both physisorption and chemisorption

**Table 3**  
Summary of studies on the application of Bz molecules as corrosion inhibitors.

Corrosion inhibitor	Substrate	Corrosive media	Corrosion inhibitor structure	Notable properties	Reference
2-Methyl-4H-benzo[d][1,3]oxazin-4-one (BZ1), and 3-amino-2-methylquinazolin-4(3H)-one (BZ2)	MS	1 M HCl		The higher inhibition efficiency (Eq. (4)) of BZ2 due to a higher tendency to donate electron. The inhibition efficiency of 51 % and 79 % for BZ1 and BZ2 at 40 °C, respectively. Chemical and physical adsorption of inhibitors to the substrate.	Kadhim et al. [69]
6-acetamido-3-benzyl-3,4-dihydro-2H-1,3-benzoxazine (ABB)	High carbon steel and Al	1 M HCl		Higher inhibition effect (Eq. (1)) of this inhibitor with high carbon steel (98 % at 40 °C) than Al (93 % at 40 °C) with corrosion.	Inbaraj et al. [71]
4-(2H-benzo[e][1,3]oxazin-3(4H)-yl)-N-(5-methyl-1,3,4-thiadiazol-2-yl)benzenesulfonamide (BSB)	Carbon steel	15 % HCl		Corrosion inhibition as the result of chemisorption and physisorption. The corrosion rate of 4.56 mm/year for ABB at 60 °C, lower than the accepted corrosion rate in acidic environments. The inhibition efficiency of 90 % at 40 °C, obtained from weight loss measurements and corrosion rate calculations.	Alamry et al. [70]

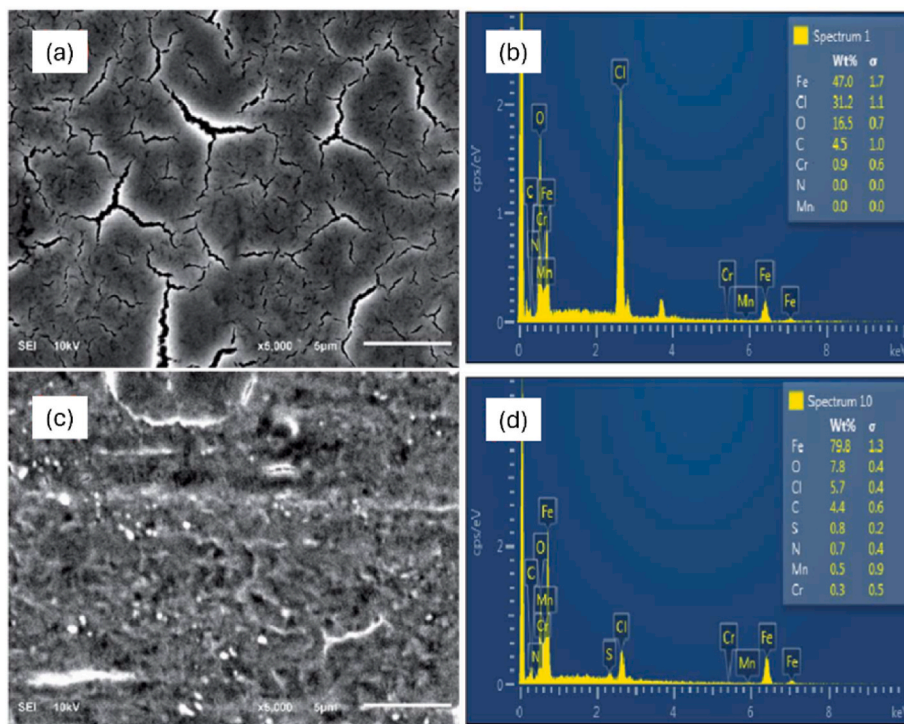


**Fig. 15.** a) SEM image, and b) EDS results for the surface of the substrate in solution without inhibitor, c) SEM image, and d) EDS results for the surface of the substrate in solution with inhibitor, after 24 h immersion in acidic solution, reproduced based on Ref. [70] with permission from the Royal Society of Chemistry.

at 40 °C for Al and different steel substrates. Table 3 presents a summary of the studies on the Bz molecule as corrosion inhibitors.

#### 4. Summary and perspectives

A brief history of Bz resin and its use as a coating was discussed. The desirable properties of pBz coatings, including thermal and chemical

stability, minimal shrinkage, and low surface free energy, arising from the unique hydrogen bonding interactions within the material, make them suitable for coating applications. Various functionalized Bz monomers were described, detailing the properties introduced by each functional group. For instance, using long flexible alkyl chains can reduce viscosity, enhance fluidity at room temperature, and increase the pBz coatings' hydrophobicity. Another influential factor contributing to

the enhanced hydrophobicity of the resulting coatings is the addition of fluorine to the backbone of the Bz monomer. The existence of fluorine groups also improves corrosion protection by increasing the cross-linking density of the pBz coating.

The curing temperature of Bz can be reduced through partial curing at lower temperatures using different curing cycles, or by increasing the number of nitrogen atoms in the structure of primary amines, which creates more cross-linking sites. Adding polyphenols and carboxylic acids also lowers the curing temperature. Cross-linking can be enhanced by incorporating other monomers, like epoxy, which increases cross-linking sites. Incorporating a silane group can lower the curing temperature of pBz, enhance adhesion to substrates through Me–O–Si bonds with metallic surfaces, and establish a dual cross-linking network that boosts hydrophobicity and barrier properties. Adding flexible segments to Bz also improves the adhesion of pBz coatings to substrates.

Copolymerization improves cross-linking density, resulting in a more robust 3D network for protecting metallic substrates from corrosion. Copolymerizing Bz monomers enhances the corrosion protection of pBz coatings by increasing both the cross-linking density and hydrophobicity. Furthermore, the application of Bz monomer as a curing agent for the epoxy coating further improves hydrophobicity and, consequently, the corrosion protection of the coating. These points are derived from previous studies; however, when analyzing data, it is crucial to consider all effective factors together, rather than in isolation. Studies showed high flexibility in the design of the Bz chemical structure, which can be modified to yield properties according to our needs.

Additives used with pBz coatings were also mentioned: carbon, SiO<sub>2</sub>, hexagonal boron nitride, benzotriazole and 2-mercaptobenzimidazole in halloysite nanotubes, and nanoclays. The critical consideration in utilizing additives is the compatibility of the additive with both the coating and the substrate. Several notable points regarding the incorporation of additives into coatings were discussed. Hexagonal boron nitride and SiO<sub>2</sub> nanoparticles can be used to create a composite coating that enhances the corrosion protection of coatings by increasing hydrophobicity. The incorporation of nanoclay into the coating effectively reduces coating porosity and alters its diffusion pathway. Additionally, two-dimensional lamellar structure polyimides function as corrosion inhibitors due to the changes in the electrolyte pathways to the substrate, thereby delaying the corrosion process.

Moreover, Bz compounds exhibit significant potential as corrosion inhibitors for Al and different steel substrates, particularly in acidic environments. Their effectiveness stems from the oxazine heterocycle, which contains electron-donating heteroatoms that enhance their inhibition efficiency. Studies have shown that increasing the concentration of these inhibitors and lowering the temperature improve their performance. The high tendency for electron donation in corrosion inhibitors is also influential in increasing the inhibition efficiency. Additionally, chemisorption and physisorption facilitate strong adhesion to metal surfaces, further enhancing corrosion resistance. The surface characterizations indicated a smooth surface without cracks and suggested the potential for protective layer formation in the presence of Bz inhibitor in the acid solution. Overall, the findings underscore the application of Bz-based inhibitors in developing sustainable and effective protective coatings for metallic substrates.

pBz coatings represent a promising advancement in sustainable materials, particularly through the development of bio-based materials derived from renewable resources. These eco-friendly alternatives significantly reduce petroleum consumption, and lower carbon emissions compared to conventional coatings. The unique properties of bio-based Bzs, such as excellent mechanical strength and thermal stability, make them suitable for diverse applications, including anticorrosion and antifouling technologies. By prioritizing non-toxic formulations and the use of renewable raw materials, pBz coatings effectively address critical environmental challenges while promoting safer and more sustainable industrial practices. The techniques used for the application of pBz coatings involve dip coating, drop coating, spray coating, spin coating,

and bar coating. To enhance their practical applicability, it is important to develop simpler and more efficient application methods, particularly those that reduce or eliminate the reliance on toxic solvents like powder coating.

Despite the considerable potential of pBz coatings as effective organic coatings, their application for lightweight metals, including Mg alloys, has not been reported and they were mostly used with steel or Al alloys substrates. Besides, due to the low thermal stability of Mg alloys, precise control of the Bz curing temperature is essential to ensure compatibility and maintain the integrity of these substrates. Optimizing these parameters will expand the applicability of pBz coatings across a wider range of industrial uses.

#### CRediT authorship contribution statement

**Roya Malekkhouyan:** Writing – original draft, Methodology, Conceptualization. **Marie-Georges Olivier:** Writing – review & editing, Validation, Supervision, Methodology, Funding acquisition, Conceptualization.

#### Declaration of competing interest

The authors declare that they have no known competing financial interests or personal relationships that could have appeared to influence the work reported in this paper.

#### Acknowledgments

This research was funded by La Fédération Wallonie-Bruxelles (Belgium) through University of MONS (UMONS), ARC 2020 (Actions de Recherche Concertées) - PROCOMAG project, Grant attributed to Roya Malekkhouyan.

#### Data availability

Data will be made available on request.

#### References

- [1] H. Ishida, T. Agag, *Handbook of Benzoxazine Resins*, Elsevier, 2011.
- [2] X.-L. Sha, S. Fang, Y. Chen, M. Zuo, Z.-H. Fei, M. Wang, Z. Liu, Synthesis and properties of low viscosity robust biobased benzoxazine resin, *React. Funct. Polym.* 194 (2024), <https://doi.org/10.1016/j.reactfunctpolym.2023.105796>.
- [3] L. Van Renterghem, R. Malekkhouyan, L. Bonnaud, R. Tavernier, M. Olivier, J.-M. Raquez, Solvent-free coatings based on bio-sourced benzoxazines resins with healing, repair, and recycling capabilities, *Prog. Org. Coating* 189 (2024), <https://doi.org/10.1016/j.porgcoat.2024.108316>.
- [4] B. Kiskan, Adapting benzoxazine chemistry for unconventional applications, *React. Funct. Polym.* 129 (2018) 76–88, <https://doi.org/10.1016/j.reactfunctpolym.2017.06.009>.
- [5] H.A. Klfout, A.M. Asiri, K.A. Alamry, M.A. Hussein, Recent advances in bio-based polybenzoxazines as an interesting adhesive coating, *RSC Adv.* 13 (29) (2023) 19817–19835, <https://doi.org/10.1039/d3ra03514j>.
- [6] R.P. Subrayan, F.N. Jones, Condensation of substituted phenols with hexakis (methoxymethyl) melamine: synthesis, characterization, and properties of substituted 2, 4, 6-tris [3, 4-dihydro-1, 3-(2 H)-benzoxazin-3-yl]-s-triazine derivatives, *Chem. Mater.* 10 (11) (1998) 3506–3512, <https://doi.org/10.1021/cm980284a>.
- [7] S. Gulyuz, B. Kiskan, Combination of polyethylenimine and vanillin-based benzoxazine as a straightforward self-healable system with excellent film-forming ability, *Macromolecules* 57 (5) (2024) 2078–2089, <https://doi.org/10.1021/acs.macromol.4c00005>.
- [8] C.H. Lin, Z.J. Chen, C.H. Chen, M.W. Wang, T.Y. Juang, Synthesis of a bisbenzylideneacetone-containing benzoxazine and its photo- and thermally cured thermoset, *ACS Omega* 2 (7) (2017) 3432–3440, <https://doi.org/10.1021/acsomega.7b00573>.
- [9] X. Wu, Y. Zhou, S.-Z. Liu, Y.-N. Guo, J.-J. Qiu, C.-M. Liu, Highly branched benzoxazine monomer based on cyclotriphosphazene: synthesis and properties of the monomer and polybenzoxazines, *Polymer* 52 (4) (2011) 1004–1012, <https://doi.org/10.1016/j.polymer.2011.01.003>.
- [10] H. Ishida, H.Y. Low, A study on the volumetric expansion of benzoxazine-based phenolic resin, *Macromolecules* 30 (4) (1997) 1099–1106, <https://doi.org/10.1021/ma960539a>.

- [11] I. Chopra, S.K. Ola, V. Dhayal, D.S. Shekhawat, Recent advances in epoxy coatings for corrosion protection of steel: experimental and modelling approach-A review, *Mater. Today Proc.* 62 (2022) 1658–1663, <https://doi.org/10.1016/j.matpr.2022.04.659>.
- [12] R. Malekkhouyan, S. Nouri Khorasani, R. Esmaeely Neisiany, R. Torkaman, M. S. Koochaki, O. Das, Preparation and characterization of electrosprayed nanocapsules containing coconut-oil-based alkyl resin for the fabrication of self-healing epoxy coatings, *Appl. Sci.* 10 (9) (2020), <https://doi.org/10.3390/app10093171>.
- [13] C.-F. Wang, Y.-C. Su, S.-W. Kuo, C.-F. Huang, Y.-C. Sheen, F.-C. Chang, Low-surface-free-energy materials based on polybenzoxazines, *Angewandte Chemie-International Edition* 45 (14) (2006) 2248–2251, <https://doi.org/10.1002/anie.200503957>.
- [14] S. Rimdusit, W. Punuch, C. Jubsilp, Effects of mono-and dianhydrides on thermal and mechanical properties enhancement of polybenzoxazine: a Property Comparison, *Appl. Mech. Mater.* 576 (2014) 63–67. <https://dx.doi.org/10.4028/www.scientific.net/AMM.576.63>.
- [15] R.-C. Lin, M.G. Mohamed, K.-C. Hsu, J.-Y. Wu, Y.-R. Jheng, S.-W. Kuo, Multivalent photo-crosslinkable coumarin-containing polybenzoxazines exhibiting enhanced thermal and hydrophobic surface properties, *Rsc Advances* 6 (13) (2016) 10683–10696, <https://doi.org/10.1039/C5RA27705A>.
- [16] M.G. Kotp, M.G. Mohamed, A.O. Mousa, S.-W. Kuo, Rational design and molecular engineering of ultrastable porous fluorescent guanidine functionalized polybenzoxazine, *Eur. Polym. J.* (2025) 113786, <https://doi.org/10.1016/j.eurpolymj.2025.113786>.
- [17] T. Agag, J. Liu, R. Graf, H.W. Spiess, H. Ishida, Benzoxazole resin: a novel class of thermoset polymer via smart benzoxazine resin, *Macromolecules* 45 (22) (2012) 8991–8997, <https://doi.org/10.1021/ma300924s>.
- [18] P. Froimowicz, K. Zhang, H. Ishida, Intramolecular hydrogen bonding in benzoxazines: when structural design becomes functional, *Chem.–Eur. J.* 22 (8) (2016) 2691–2707, <https://doi.org/10.1002/chem.201503477>.
- [19] X. Ning, H. Ishida, Phenolic materials via ring-opening polymerization of benzoxazines: effect of molecular structure on mechanical and dynamic mechanical properties, *J. Polym. Sci. B Polym. Phys.* 32 (5) (1994) 921–927, <https://doi.org/10.1002/polb.1994.090320515>.
- [20] Y. Zhou, G. Wei, J. Yuan, X. Sang, J.-T. Miao, R. Liu, UV-assisted direct ink writing 4D printing of benzoxazine/epoxy thermosets, *Chem. Eng. J.* 477 (2023), <https://doi.org/10.1016/j.cej.2023.147221>.
- [21] D. Iguchi, S. Ohashi, G.J. Abarro, X. Yin, S. Winthro, C. Scott, M. Gleydura, L. Jin, N. Kanagasagar, C. Lo, Development of hydrogen-rich benzoxazine resins with low polymerization temperature for space radiation shielding, *ACS Omega* 3 (9) (2018) 11569–11581, <https://doi.org/10.1021/acsomega.8b01297>.
- [22] S. Rimdusit, H. Ishida, Development of new class of electronic packaging materials based on ternary systems of benzoxazine, epoxy, and phenolic resins, *Polymer* 41 (22) (2000) 7941–7949, [https://doi.org/10.1016/S0032-3861\(00\)00164-00166](https://doi.org/10.1016/S0032-3861(00)00164-00166).
- [23] G.-P. Hao, W.-C. Li, D. Qian, G.-H. Wang, W.-P. Zhang, T. Zhang, A.-Q. Wang, F. Schuth, H.-J. Bongard, A.-H. Lu, Structurally designed synthesis of mechanically stable poly (benzoxazine-co-resol)-based porous carbon monoliths and their application as high-performance CO<sub>2</sub> capture sorbents, *J. Am. Chem. Soc.* 133 (29) (2011) 11378–11388, <https://doi.org/10.1021/ja203857g>.
- [24] R. Konnola, T.S. Anirudhan, Efficient carbon dioxide capture by nitrogen and sulfur dual-doped mesoporous carbon spheres from polybenzoxazines synthesized by a simple strategy, *J. Environ. Chem. Eng.* 8 (1) (2020) 103614, <https://doi.org/10.1016/j.jece.2019.103614>.
- [25] X. Chen, Q. Li, T. Zhang, Y. Zhen, T. Li, Y. Zhu, B. Ti, Benzoxazine/thermoplastic polyurethane nanofibrous membranes with superior mechanical properties for efficient oil-water separation, *J. Membr. Sci.* 702 (2024) 122788, <https://doi.org/10.1016/j.memsci.2024.122788>.
- [26] M.G. Mohamed, B.-X. Su, S.-W. Kuo, Robust nitrogen-doped microporous carbon via crown ether-functionalized benzoxazine-linked porous organic polymers for enhanced CO<sub>2</sub> adsorption and supercapacitor applications, *ACS Appl. Mater. Interfaces* 16 (31) (2024) 40858–40872, <https://doi.org/10.1021/acsami.4c05645>.
- [27] M. Ejaz, M.G. Mohamed, Y.-T. Chen, K. Zhang, S.-W. Kuo, Porous carbon materials augmented with heteroatoms derived from hyperbranched biobased benzoxazine resins for enhanced CO<sub>2</sub> adsorption and exceptional supercapacitor Performance, *J. Energy Storage* 78 (2024) 110166, <https://doi.org/10.1016/j.est.2023.110166>.
- [28] M.G. Mohamed, W.-C. Chang, S.-W. Kuo, Crown ether-and benzoxazine-linked porous organic polymers displaying enhanced metal ion and CO<sub>2</sub> capture through solid-state chemical transformation, *Macromolecules* 55 (17) (2022) 7879–7892, <https://doi.org/10.1021/acs.macromol.2c01216>.
- [29] M. Ejaz, M.G. Mohamed, W.-C. Huang, Y.-C. Kao, W.-C. Chen, S.-W. Kuo, Highly thermally stable polyhedral oligomeric silsesquioxane based on diacetal-functionalized polybenzoxazine nanocomposites, *Eur. Polym. J.* 223 (2025) 113649, <https://doi.org/10.1016/j.eurpolymj.2024.113649>.
- [30] M. Phagare, Benzoxazine resin market report 2024 (global edition), 8th: [Available from: <https://www.cognitivemarketresearch.com/benzoxazine-resin-market-report>, 2023 March 2024.
- [31] A. Candia, M.E. Taverna, A. Forchetti Casarino, C. Busatto, N. Casis, M. E. Spontón, J. La Scala, D. Estenez, Lignosulfonate/silica hybrid nanoparticles as a novel biobased filler in polybenzoxazine matrix, *Polym. Adv. Technol.* 35 (3) (2024), <https://doi.org/10.1002/pat.6342>.
- [32] M. Wang, D. Han, J. Jiang, T. Bu, Z. Wang, Enhancing comprehensive performances of polybenzoxazine through integration of soft core–soft shell cellulose-based nanoparticles, *Polym. Compos.* (2024), <https://doi.org/10.1002/pc.28424>.
- [33] N. Ramdani, M. Derradji, E.O. Mokhnache, Natural fiber reinforced polybenzoxazine composites: a review, *Mater. Today Commun.* 31 (2022), <https://doi.org/10.1016/j.mtcomm.2022.103645>.
- [34] K.I. Aly, M.G. Mohamed, O. Younis, M.H. Mahross, M. Abdel-Hakim, M.M. Sayed, Salicylaldehyde azine-functionalized polybenzoxazine: synthesis, characterization, and its nanocomposites as coatings for inhibiting the mild steel corrosion, *Prog. Org. Coating* 138 (2020), <https://doi.org/10.1016/j.porgcoat.2019.105385>.
- [35] A. Rucigaj, B. Alic, M. Krajnc, U. Sebenik, Curing of bisphenol A-aniline based benzoxazine using phenolic, amino and mercapto accelerators, *Express Polym. Lett.* 9 (7) (2015) 647–657, <https://doi.org/10.3144/expresspolymlett.2015.60>.
- [36] T. Periyasamy, S.P. Asrafali, S.-C. Kim, Bio-based polybenzoxazine–cellulose grafted films: material fabrication and properties, *Polymers* 15 (4) (2023) 849, <https://doi.org/10.3390/polym15040849>.
- [37] A. Adjaoud, A. Trejo-Machin, L. Puchot, P. Verge, Polybenzoxazines: a sustainable platform for the design of fast responsive and catalyst-free vitrimers based on trans-esterification exchanges, *Polym. Chem.* 12 (22) (2021) 3276–3289, <https://doi.org/10.1039/d1py00324k>.
- [38] Z. Wen, L. Bonnaud, R. Mincheva, P. Dubois, J.-M. Raquez, Development of low-viscosity and high-performance biobased monobenzoxazine from tyrosol and furfurylamine, *Materials* 14 (2) (2021) 440, <https://doi.org/10.3390/ma14020440>.
- [39] L. Bonnaud, B. Chollet, L. Dumas, A.A. Peru, A.L. Flourat, F. Allais, P. Dubois, High-performance bio-based benzoxazines from enzymatic synthesis of diphenols, *Macromol. Chem. Phys.* 220 (1) (2019) 1800312, <https://doi.org/10.1002/macp.201800312>.
- [40] A. Tuzun, B. Kiskan, N. Alemdar, A.T. Erciyi, Y. Yagci, Benzoxazine containing polyester thermosets with improved adhesion and flexibility, *J. Polym. Sci. Polym. Chem.* 48 (19) (2010) 4279–4284, <https://doi.org/10.1002/pola.24215>.
- [41] X. Lu, Y. Liu, C. Zhou, W. Zhang, Z. Xin, Corrosion protection of hydrophobic bisphenol A-based polybenzoxazine coatings on mild steel, *RSC advances* 6 (7) (2016) 5805–5811, <https://doi.org/10.1039/C5RA22980D>.
- [42] H.P. Higginbottom, Polymerizable compositions comprising polyamines and poly (dihydrobenzoxazines), U.S. Pat. 4501864, <https://patents.google.com/patent/US4501864A/en>, 1985.
- [43] A.M.M. Soliman, K.I. Aly, M.G. Mohamed, A.A. Amer, M.R. Belal, M. Abdel-Hakim, Synthesis, characterization and protective efficiency of novel polybenzoxazine precursor as an anticorrosive coating for mild steel, *Sci. Rep.* 13 (1) (2023) 5581, <https://doi.org/10.1038/s41598-023-30364-x>.
- [44] A. Mahdy, K.I. Aly, M.G. Mohamed, Construction novel polybenzoxazine coatings exhibiting corrosion protection of mild steel at different concentrations in a seawater solution, *Heliyon* 9 (7) (2023) e17977, <https://doi.org/10.1016/j.heliyon.2023.e17977>.
- [45] K.I. Aly, A. Mahdy, M.A. Hegazy, N.S. Al-Muaiikel, S.-W. Kuo, M. Gamal Mohamed, Corrosion resistance of mild steel coated with phthalimide-functionalized polybenzoxazines, *Coatings* 10 (11) (2020), <https://doi.org/10.3390/coatings10111114>.
- [46] K.I. Aly, A.A. Amer, M.H. Mahross, M.R. Belal, A.M.M. Soliman, M.G. Mohamed, Construction of novel polybenzoxazine coating precursor exhibiting excellent anti-corrosion performance through monomer design, *Heliyon* 9 (5) (2023) e15976, <https://doi.org/10.1016/j.heliyon.2023.e15976>.
- [47] M.G. Mohamed, A. Mahdy, R.J. Obaid, M.A. Hegazy, S.-W. Kuo, K.I. Aly, Synthesis and characterization of polybenzoxazine/clay hybrid nanocomposites for UV light shielding and anti-corrosion coatings on mild steel, *J. Polym. Res.* 28 (8) (2021), <https://doi.org/10.1007/s10965-021-02657-0>.
- [48] X. Chen, X. Zhang, J. Chen, W. Bai, X. Zheng, Q. Lin, F. Lin, Y. Xu, Two-dimensional lamellar polyimide/cardanol-based benzoxazine copper polymer composite coatings with excellent anti-corrosion performance, *RSC Adv.* 12 (17) (2022) 10766–10777, <https://doi.org/10.1039/d1ra08844k>.
- [49] A. Suesuwan, N. Suetrong, S. Yaemphutthong, I. Tiewlamsam, K. Chansaenpak, S. Wannapaiboon, N. Chuanapparat, L. Srathongsian, P. Kanjanaboos, N. Chanthaset, W. Wattananathana, Partially bio-based benzoxazine monomers derived from thymol: photoluminescent properties, polymerization characteristics, hydrophobic coating investigations, and anticorrosion studies, *Polymers* 16 (13) (2024), <https://doi.org/10.3390/polym16131767>.
- [50] M.G. Mohamed, C.-J. Li, M.A.R. Khan, C.-C. Liaw, K. Zhang, S.-W. Kuo, Formaldehyde-free synthesis of fully bio-based multifunctional bisbenzoxazine resins from natural renewable starting materials, *Macromolecules* 55 (8) (2022) 3106–3115, <https://doi.org/10.1021/acs.macromol.2c00417>.
- [51] Z. Qian, Q. Li, L. Wang, F. Fu, X. Liu, The chemical effect of furfuryl amide on the enhanced performance of the diphenolic acid derived bio-polybenzoxazine resin, *J. Polym. Sci.* 59 (18) (2021) 2057–2068, <https://doi.org/10.1002/pol.20210399>.
- [52] X. Liu, R. Zhang, T. Li, P. Zhu, Q. Zhuang, Novel fully biobased benzoxazines from rosin: synthesis and properties, *ACS Sustain. Chem. Eng.* 5 (11) (2017) 10682–10692, <https://doi.org/10.1021/acsuschemeng.7b02650>.
- [53] C. Wang, J. Sun, X. Liu, A. Sudo, T. Endo, Synthesis and copolymerization of fully bio-based benzoxazines from guaiacol, furfurylamine and stearylamine, *Green Chem.* 14 (10) (2012) 2799–2806, <https://doi.org/10.1039/C2GC35796H>.
- [54] K. Mohamed Mydeen, H. Arumugam, B. Krishnasamy, S. Sathy Srikandan, A. Muthukaruppan, Sustainable l-tyrosine based bio-benzoxazines for efficient protection of mild steel surfaces from marine environment, *Int. J. Adhesion Adhes.* 125 (2023), <https://doi.org/10.1016/j.ijadhadh.2023.103405>.

- [55] N. Sini, J. Bijiwe, I.K. Varma, Renewable benzoxazine monomer from Vanillin: synthesis, characterization, and studies on curing behavior, *J. Polym. Sci. Polym. Chem. Ed.* 52 (1) (2014) 7–11, <https://doi.org/10.1002/pola.26981>.
- [56] A. Van, K. Chiou, H. Ishida, Use of renewable resource vanillin for the preparation of benzoxazine resin and reactive monomeric surfactant containing oxazine ring, *Polymer* 55 (6) (2014) 1443–1451, <https://doi.org/10.1016/j.polymer.2014.01.041>.
- [57] S. Appasamy, B. Krishnasamy, S. Ramachandran, A. Muthukaruppan, Vanillin derived partially bio-based benzoxazine resins for hydrophobic coating and anticorrosion applications: studies on syntheses and thermal behavior, *Polymer-Plastics Technology and Materials* 63 (3) (2024) 287–298, <https://doi.org/10.1080/25740881.2023.2283772>.
- [58] N. Salahuddin, A. Rehab, I.Y. El-Deeb, R. Elmokadem, Effect of graphene oxide on photo- and thermal curing of chalcone-based benzoxazine resins, *Polym. Bull.* (2022) 1–17, <https://doi.org/10.1007/s00289-021-03590-4>.
- [59] P. Madesh, B. Krishnasamy, H. Arumugam, A. Muthukaruppan, Role of magnolol embedded fully bio-based benzoxazines for hydrophobic, anti-microbial and anti-corrosion applications, *New J. Chem.* 48 (8) (2024) 3456–3466, <https://doi.org/10.1039/D3NJ05576K>.
- [60] L. Dumas, L. Bonnaud, M. Olivier, M. Poorteman, P. Dubois, Bio-based high performance thermosets: stabilization and reinforcement of eugenol-based benzoxazine networks with BMI and CNT, *Eur. Polym. J.* 67 (2015) 494–502, <https://doi.org/10.1016/j.eurpolymj.2014.11.030>.
- [61] L. Dumas, L. Bonnaud, M. Olivier, M. Poorteman, P. Dubois, Eugenol-based benzoxazine: from straight synthesis to taming of the network properties, *J. Mater. Chem. A* 3 (11) (2015) 6012–6018, <https://doi.org/10.1039/C4TA06636G>.
- [62] X. Liu, Z. Li, G. Zhan, Y. Wu, Q. Zhuang, Bio-based benzoxazines based on sesamol: synthesis and properties, *J. Appl. Polym. Sci.* 136 (48) (2019) 48255, <https://doi.org/10.1002/app.48255>.
- [63] W. Zhao, B. Chen, K. Zhang, Biobased bisbenzoxazine resins derived from natural renewable monophenols and diamine: synthesis and property investigations, *ACS Sustain. Chem. Eng.* 10 (45) (2022) 14783–14793, <https://doi.org/10.1021/acsschemeng.2c04103>.
- [64] L. Dumas, L. Bonnaud, M. Olivier, M. Poorteman, P. Dubois, Chavicol benzoxazine: ultrahigh Tg biobased thermoset with tunable extended network, *Eur. Polym. J.* 81 (2016) 337–346, <https://doi.org/10.1016/j.eurpolymj.2016.06.018>.
- [65] P. Froimowicz, C. R. Arza, L. Han, H. Ishida, Smart, sustainable, and ecofriendly chemical design of fully bio-based thermally stable thermosets based on benzoxazine chemistry, *ChemSusChem* 9 (15) (2016) 1921–1928, <https://doi.org/10.1002/cssc.201600577>.
- [66] B. Rao, A. Palanisamy, Monofunctional benzoxazine from cardanol for bio-composite applications, *React. Funct. Polym.* 71 (2) (2011) 148–154, <https://doi.org/10.1016/j.reactfunctpolym.2010.11.025>.
- [67] P. Madesh, S. Ramachandran, B. Krishnasamy, A. Muthukaruppan, Synthesis of a new type of bisphenol-BC-based benzoxazines from sustainable bio-phenol for hydrophobic, dielectric and corrosion-resistant applications, *J. Macromol. Sci., Part A* 61 (3) (2024) 203–212, <https://doi.org/10.1080/10601325.2024.2322437>.
- [68] Y. Lu, K. Zhang, Synthesis and properties of biobased mono-benzoxazine resins from natural renewable pterostilbene, *Eur. Polym. J.* 156 (2021) 110607, <https://doi.org/10.1016/j.eurpolymj.2021.110607>.
- [69] A. Kadhim, A.K. Al-Okbi, D.M. Jamil, A. Qussay, A.A. Al-Amri, T.S. Gaaz, A.A. H. Kadhum, A.B. Mohamad, M.H. Nassir, Experimental and theoretical studies of benzoxazines corrosion inhibitors, *Results Phys.* 7 (2017) 4013–4019, <https://doi.org/10.1016/j.rinp.2017.10.027>.
- [70] K.A. Alamry, M.A. Hussein, A. Musa, K. Haruna, T.A. Saleh, The inhibition performance of a novel benzenesulfonamide-based benzoxazine compound in the corrosion of X60 carbon steel in an acidizing environment, *RSC Adv.* 11 (12) (2021) 7078–7095, <https://doi.org/10.1039/d0ra10317a>.
- [71] N. Ugin Inbaraj, G. Venkatesa Prabhhu, Corrosion inhibition properties of paracetamol based benzoxazine on HCS and Al surfaces in 1M HCl, *Prog. Org. Coating* 115 (2018) 27–40, <https://doi.org/10.1016/j.porgcoat.2017.11.007>.
- [72] B. Vaghefinazari, E. Wierzbicka, P. Visser, R. Posner, R. Arrabal, E. Matykina, M. Mohedano, C. Blawert, M.L. Zheludkevich, S.V. Lamaka, Chromate-free corrosion protection strategies for magnesium alloys-A review: Part III-corrosion inhibitors and combining them with other protection strategies, *Materials* 15 (23) (2022), <https://doi.org/10.3390/ma15238489>.
- [73] X. Zhou, Q. Dong, D. Wei, J. Bai, F. Xue, B. Zhang, Z. Ba, Z. Wang, Smart corrosion inhibitors for controlled release: a review, *Corrosion Eng. Sci. Technol.* 58 (2) (2022) 190–204, <https://doi.org/10.1080/1478422x.2022.2161122>.
- [74] B.C. Sahu, Organic corrosion inhibitors, in: *Introduction to Corrosion-Basics and Advances*, IntechOpen, 2023.
- [75] X. Zhu, C. Wang, Corrosion inhibition performance of an environmentally friendly water-based nano-inhibitor, *Alex. Eng. J.* 70 (2023) 495–501, <https://doi.org/10.1016/j.aej.2023.03.013>.
- [76] D.M. Patil, G.A. Phalak, S. Mhaske, Synthesis and characterization of bio-based benzoxazine oligomer from cardanol for corrosion resistance application, *J. Coating Technol. Res.* 14 (2017) 517–530, <https://doi.org/10.1007/s11998-016-9892-3>.
- [77] F. Wu, J. Liang, Z. Peng, B. Liu, Electrochemical deposition and characterization of Zn-Al layered double hydroxides (LDHs) films on magnesium alloy, *Appl. Surf. Sci.* 313 (2014) 834–840, <https://doi.org/10.1016/j.apsusc.2014.06.083>.
- [78] R. Malekkhouyan, Y. Paint, L. Prince, M. Gonon, M.-G. Olivier, Controlling lateral size and thickness of layered double hydroxide (LDH) used as conversion layer for corrosion protection of AZ31 Mg alloy, *Corrosion and Materials Degradation* 4 (1) (2023) 174–195, <https://doi.org/10.3390/cmd4010011>.
- [79] A. Hariharan, M. Kesava, M. Alagar, K. Dinakaran, K. Subramanian, Optical, electrochemical, and thermal behavior of polybenzoxazine copolymers incorporated with tetraphenylimidazole and diphenylquinoline, *Polym. Adv. Technol.* 29 (1) (2018) 355–363, <https://doi.org/10.1002/pat.4122>.
- [80] M. Ariraman, M. Alagar, Studies on dielectric properties of GO reinforced bisphenol-Z polybenzoxazine hybrids, *Rsc Advances* 5 (30) (2015) 23787–23797, <https://doi.org/10.1039/C5RA00472A>.
- [81] A. Hariharan, K. Srinivasan, C. Murthy, M. Alagar, Synthesis and characterization of a novel class of low temperature cure Benzoxazines, *J. Polym. Res.* 25 (2018) 1–13, <https://doi.org/10.1007/s10965-017-1423-0>.
- [82] H. Okada, T. Tokunaga, X. Liu, S. Takayanagi, A. Matsushima, Y. Shimohigashi, Direct evidence revealing structural elements essential for the high binding ability of bisphenol A to human estrogen-related receptor- $\gamma$ , *Environmental health perspectives* 116 (1) (2008) 32–38, <https://doi.org/10.1289/ehp.10587>.
- [83] J.R. Rochester, A.L. Bolden, Bisphenol S and F: a systematic review and comparison of the hormonal activity of bisphenol A substitutes, *Environmental health perspectives* 123 (7) (2015) 643–650, <https://doi.org/10.1289/ehp.140898>.
- [84] J. da Silva Santos, M. da Silva Pontes, M.B. de Souza, S.Y. Fernandes, R. A. Azevedo, G.J. de Arruda, E.F. Santiago, Toxicity of bisphenol A (BPA) and its analogues BPF and BPS on the free-floating macrophyte *Salvinia biloba*, *Chemosphere* 343 (2023) 140235, <https://doi.org/10.1016/j.chemosphere.2023.140235>.
- [85] M. Manoj, A. Kumaravel, R. Mangalam, P. Prabunathan, A. Hariharan, M. Alagar, Exploration of high corrosion resistance property of less hazardous pyrazolidine-based benzoxazines in comparison with bisphenol-F derivatives, *J. Coating Technol. Res.* 17 (4) (2020) 921–935, <https://doi.org/10.1007/s11998-019-00312-4>.
- [86] S. Krishnan, H. Arumugam, C. Kuppan, A. Goswami, M. Chavali, A. Muthukaruppan, Silane-functionalized polybenzoxazines: a superior corrosion resistant coating for steel plates, *Mater. Corros.* 68 (12) (2017) 1343–1354, <https://doi.org/10.1002/maco.201709587>.
- [87] J. Escobar, M. Poorteman, L. Dumas, L. Bonnaud, P. Dubois, M.-G. Olivier, Thermal curing study of bisphenol A benzoxazine for barrier coating applications on 1050 aluminum alloy, *Prog. Org. Coating* 79 (2015) 53–61, <https://doi.org/10.1016/j.porgcoat.2014.11.004>.
- [88] A. Renaud, M. Poorteman, J. Escobar, L. Dumas, Y. Paint, L. Bonnaud, P. Dubois, M.-G. Olivier, A new corrosion protection approach for aeronautical applications combining a Phenol-paraPhenyleneDiAmine benzoxazine resin applied on sulfotartaric anodized aluminum, *Prog. Org. Coating* 112 (2017) 278–287, <https://doi.org/10.1016/j.porgcoat.2017.07.007>.
- [89] A. Renaud, Y. Paint, A. Lanzutti, L. Bonnaud, L. Fedrizzi, P. Dubois, M. Poorteman, M.G. Olivier, Sealing porous anodic layers on AA2024-T3 with a low viscosity benzoxazine resin for corrosion protection in aeronautical applications, *RSC Adv.* 9 (29) (2019) 16819–16830, <https://doi.org/10.1039/c9ra01970g>.
- [90] M.G. Mohamed, S.W. Kuo, Functional polyimide/polyhedral oligomeric silsesquioxane nanocomposites, *Polymers* 11 (1) (2018) 26, <https://doi.org/10.3390/polym11010026>.
- [91] K. Vanherck, G. Koeckelberghs, I.F. Vankelecom, Crosslinking polyimides for membrane applications: a review, *Prog. Polym. Sci.* 38 (6) (2013) 874–896, <https://doi.org/10.1016/j.progpolymsci.2012.11.001>.
- [92] K.F. Hamak, Synthetic of Phthalimides via the reaction of phthalic anhydride with amines and evaluating of its biological and anti corrosion activity, *Int. J. Chemtech. Res.* 6 (1) (2014) 324–333.
- [93] C. Li, Z. Zhou, S. Lin, X. Meng, J. Liu, C. Zhou, Studying how changes in the structure caused by hydrogen bonding affect the corrosion resistance of polybenzoxazine-based coatings using molecular dynamics simulations, *Prog. Org. Coating* 192 (2024), <https://doi.org/10.1016/j.porgcoat.2024.108475>.
- [94] N. Parhizkar, B. Ramezanzadeh, T. Shahrabi, Corrosion protection and adhesion properties of the epoxy coating applied on the steel substrate pre-treated by a sol-gel based silane coating filled with amino and isocyanate silane functionalized graphene oxide nanosheets, *Appl. Surf. Sci.* 439 (2018) 45–59, <https://doi.org/10.1016/j.apsusc.2017.12.240>.
- [95] J. Liu, X. Lu, Z. Xin, C.-I. Zhou, Surface properties and hydrogen bonds of mono-functional polybenzoxazines with different N-substituents, *Chin. J. Polym. Sci.* 34 (8) (2016) 919–932, <https://doi.org/10.1007/s10118-016-1810-8>.
- [96] M. Mydeen, B. Krishnasamy, A. Rajamani, A. Muthukaruppan, Sustainable furfural bis-thymol based benzoxazines: superhydrophobic, aggregation induced emission and corrosion resistant properties, *J. Mol. Struct.* 1322 (2025) 140495, <https://doi.org/10.1016/j.molstruc.2024.140495>.
- [97] H. Srinivasan, H. Arumugam, B. Krishnasamy, K.S. Mani, A. Muthukaruppan, High-potent trifunctional polybenzoxazines coatings for superhydrophobic cotton fabrics and mild steel corrosion protection applications, *J. Appl. Polym. Sci.* 141 (25) (2024), <https://doi.org/10.1002/app.55540>.
- [98] A. Suesuwan, N. Suetrong, S. Yaemphutthong, I. Tiewlamsam, K. Chansaenpak, S. Wannapaiboon, N. Chuanopparat, L. Srathongsian, P. Kanjanaboos, N. Chanthaset, W. Wattananathana, Partially bio-based benzoxazine monomers derived from thymol: photoluminescent properties, polymerization characteristics, hydrophobic coating investigations, and anticorrosion studies, *Polymers* 16 (13) (2024), <https://doi.org/10.3390/polym16131767>.
- [99] G. Khan, W.J. Basirun, S.N. Kazi, P. Ahmed, L. Magaji, S.M. Ahmed, G.M. Khan, M.A. Rehman, A.B.B.M. Badry, Electrochemical investigation on the corrosion inhibition of mild steel by Quinazoline Schiff base compounds in hydrochloric

- acid solution, *J. Colloid Interface Sci.* 502 (2017) 134–145, <https://doi.org/10.1016/j.jcis.2017.04.061>.
- [100] P. Krishnan, P. Madesh, B. Krishnasamy, R. Thamizselvi, A. Muthukaruppan, Multifunctional nitrogen rich benzoxazines with imine moiety: structural insights, hydrophobic and corrosion-resistant applications, *J. Appl. Polym. Sci.* 141 (45) (2024) e56203, <https://doi.org/10.1002/app.56203>.
- [101] N. Muthukumar, H. Arumugam, B. Krishnasamy, M. Athianna, A. Muthukaruppan, Synthesis and characterization of sustainable curcumin-based bio-benzoxazines for antimicrobial and anticorrosion applications, *ChemistrySelect* 8 (12) (2023), <https://doi.org/10.1002/slct.202204302>.
- [102] C.J. Raorane, T. Periyasamy, R. Haldhar, S.P. Asrafali, V. Raj, S.C. Kim, Synthesis of bio-based polybenzoxazine and its antibiofilm and anticorrosive activities, *Materials* 16 (6) (2023), <https://doi.org/10.3390/ma16062249>.
- [103] T. Periyasamy, S.P. Asrafali, C.J. Raorane, V. Raj, D. Shastri, S.C. Kim, Sustainable chitosan/polybenzoxazine films: synergistically improved thermal, mechanical, and antimicrobial properties, *Polymers* 15 (4) (2023), <https://doi.org/10.3390/polym15041021>.
- [104] P. Madesh, H. Arumugam, B. Krishnasamy, A. Muthukaruppan, Synthesis of sustainable curcumin based photo-crosslinkable benzoxazines: thermal, hydrophobic and anti-corrosion properties, *J. Mol. Struct.* 1296 (2024) 136902, <https://doi.org/10.1016/j.molstruc.2023.136902>.
- [105] G.A. Phalal, D.M. Patil, S.T. Mhaske, Synthesis and characterization of thermally curable guaiacol based poly(benzoxazine-urethane) coating for corrosion protection on mild steel, *Eur. Polym. J.* 88 (2017) 93–108, <https://doi.org/10.1016/j.eurpolymj.2016.12.030>.
- [106] J. Liu, J. Dai, S. Wang, Y. Peng, L. Cao, X. Liu, Facile synthesis of bio-based reactive flame retardant from vanillin and guaiacol for epoxy resin, *Compos. B Eng.* 190 (2020) 107926, <https://doi.org/10.1016/j.compositesb.2020.107926>.
- [107] R.W. Holley, J. Apgar, B. Doctor, J. Farrow, M.A. Marini, S.H. Merrill, A simplified procedure for the preparation of tyrosine-and valine-acceptor fractions of yeast “soluble ribonucleic acid”, *J. Biol. Chem.* 236 (1) (1961) 200–202, [https://doi.org/10.1016/S0021-9258\(18\)64455-2](https://doi.org/10.1016/S0021-9258(18)64455-2).
- [108] S. Ren, F. Tian, S. Zhang, W. Zhou, Y. Du, Bio-based benzoxazine from renewable L-tyrosine: synthesis, polymerization, and properties, *J. Polym. Sci.* 60 (9) (2022) 1492–1500, <https://doi.org/10.1002/pol.20210786>.
- [109] A. Adjaoud, L. Puchot, C.E. Federico, R. Das, P. Verge, Lignin-based benzoxazines: a tunable key-precursor for the design of hydrophobic coatings, fire resistant materials and catalyst-free vitrimers, *Chem. Eng. J.* 453 (2023) 139895, <https://doi.org/10.1016/j.cej.2022.139895>.
- [110] C. Scarica, R. Suriano, M. Levi, S. Turri, G. Griffini, Lignin functionalized with succinic anhydride as building block for biobased thermosetting polyester coatings, *ACS Sustain. Chem. Eng.* 6 (3) (2018) 3392–3401, <https://doi.org/10.1021/acsschemeng.7b03583>.
- [111] V. Selvaraj, K. Jayanthi, M. Alagar, Development of biocomposites from agro wastes for low dielectric applications, *J. Polym. Environ.* 26 (2018) 3655–3669, <https://doi.org/10.1039/C9RA08741A>.
- [112] V.S. Balachandran, S.R. Jadhav, P.K. Vemula, G. John, Recent advances in cardanol chemistry in a nutshell: from a nut to nanomaterials, *Chem. Soc. Rev.* 42 (2) (2013) 427–438, <https://doi.org/10.1039/C2CS35344J>.
- [113] P. Jia, F. Song, Q. Li, H. Xia, M. Li, X. Shu, Y. Zhou, Recent development of cardanol based polymer materials-a review, *Journal of Renewable Materials* 7 (7) (2019) 601–619, <https://doi.org/10.32604/jrm.2019.07011>.
- [114] S. Shukla, A. Mahata, B. Pathak, B. Lochab, Cardanol benzoxazines–interplay of oxazine functionality (mono to tetra) and properties, *RSC advances* 5 (95) (2015) 78071–78080, <https://doi.org/10.1039/C5RA14214H>.
- [115] M. Monisha, N. Amarnath, S. Mukherjee, B. Lochab, Cardanol benzoxazines: a versatile monomer with advancing applications, *Macromol. Chem. Phys.* 220 (3) (2019) 1800470, <https://doi.org/10.1002/macp.201800470>.
- [116] E. Bloise, L. Carbone, G. Colafemmina, L. D'Accolti, S.E. Mazzetto, G. Vasapollo, G. Mele, First example of a lipophilic porphyrin-cardanol hybrid embedded in a cardanol-based micellar nanodispersion, *Molecules* 17 (10) (2012) 12252–12261, <https://doi.org/10.3390/molecules171012252>.
- [117] L. Wang, M. Yuan, Y. Zhao, Z. Guo, X. Lu, Z. Xin, Fabrication of superhydrophobic bio-based polybenzoxazine/hexagonal boron nitride composite coating for corrosion protection, *Prog. Org. Coating* 167 (2022), <https://doi.org/10.1016/j.porgcoat.2022.106863>.
- [118] R. Andreu, J. Reina, J. Ronda, Carboxylic acid-containing benzoxazines as efficient catalysts in the thermal polymerization of benzoxazines, *J. Polym. Sci. Polym. Chem.* 46 (18) (2008) 6091–6101, <https://doi.org/10.1002/pola.22921>.
- [119] J. Ye, X. Lu, Z. Xin, Cardanol-based polybenzoxazine coatings: crosslinking structures, hydrophobicity and corrosion protection properties, *J. Polym. Sci.* 62 (13) (2024) 2936–2944, <https://doi.org/10.1002/pol.20240139>.
- [120] Z. Li, P. Liu, S. Chen, X. Liu, Y. Yu, T. Li, Y. Wan, N. Tang, Y. Liu, Y. Gu, Bioinspired marine antifouling coatings: antifouling mechanisms, design strategies and application feasibility studies, *Eur. Polym. J.* 190 (2023) 111997, <https://doi.org/10.1016/j.eurpolymj.2023.111997>.
- [121] J. Pan, L. Mei, H. Zhou, C. Zhang, Q. Xie, C. Ma, Self-regenerating zwitterionic hyperbranched polymer with tunable degradation for anti-biofouling coatings, *Prog. Org. Coating* 163 (2022) 106674, <https://doi.org/10.1016/j.porgcoat.2021.106674>.
- [122] J. Chen, W. Bai, R. Jian, Y. Lin, X. Zheng, F. Wei, Q. Lin, F. Lin, Y. Xu, Molecular structure design of polybenzoxazines with low surface energy and low modulus for marine antifouling application, *Prog. Org. Coating* 187 (2024), <https://doi.org/10.1016/j.porgcoat.2023.108165>.
- [123] J. Chen, J. Zhao, F. Lin, X. Zheng, R. Jian, Y. Lin, F. Wei, Q. Lin, W. Bai, Y. Xu, Polymerized tung oil toughened urushiol-based benzoxazine copper polymer coatings with excellent antifouling performances, *Prog. Org. Coating* 177 (2023), <https://doi.org/10.1016/j.porgcoat.2023.107411>.
- [124] Y. Zhang, X. Liu, G. Zhan, Q. Zhuang, R. Zhang, J. Qian, Study on the synergistic anticorrosion property of a fully bio-based polybenzoxazine copolymer resin, *Eur. Polym. J.* 119 (2019) 477–486, <https://doi.org/10.1016/j.eurpolymj.2019.07.020>.
- [125] C. Chen, Y. Cao, X. Lu, X. Li, H. Yao, Z. Xin, Copolymer of eugenol-based and pyrogallol-based benzoxazines: low curing temperature and enhanced corrosion resistance, *Colloids Surf. A Physicochem. Eng. Asp.* 609 (2021) 125605, <https://doi.org/10.1016/j.colsurfa.2020.125605>.
- [126] C. Zhao, J. Wei, J. Wu, Y. Li, D. Xiang, Y. Wu, H. Li, Z. Hou, Synthesis and characterization of polyetheramine-type benzoxazines as protective coatings for low carbon steel against corrosion in sodium chloride solution, *Int. J. Electrochem. Sci.* 17 (6) (2022), <https://doi.org/10.20964/2022.06.43>.
- [127] C. Zhou, X. Lu, Z. Xin, J. Liu, Corrosion resistance of novel silane-functional polybenzoxazine coating on steel, *Corros. Sci.* 70 (2013) 145–151, <https://doi.org/10.1016/j.corsci.2013.01.023>.
- [128] P. Sharma, P. Dutta, L. Nebhani, Sustainable approach towards enhancing thermal stability of bio-based polybenzoxazines, *Polymer* 184 (2019) 121905, <https://doi.org/10.1016/j.polymer.2019.121905>.
- [129] L. Qu, Z. Xin, Preparation and surface properties of novel low surface free energy fluorinated silane-functional polybenzoxazine films, *Langmuir* 27 (13) (2011), <https://doi.org/10.1021/la200073v>, pp. 8365–70.
- [130] Z. Zhou, C. Li, R. Wang, H. Tao, D. Yang, S. Qin, X. Meng, C. Zhou, Crosslinking control of hydrophobic benzoxazine-based hybrid sol-gel coating for corrosion protection on aluminum alloys, *Prog. Org. Coating* 171 (2022), <https://doi.org/10.1016/j.porgcoat.2022.107059>.
- [131] Z. Zhou, J. Liu, X. Meng, C. Zhou, Improved corrosion resistance and hydrophobic stability of sol-gel coatings by benzoxazine modification on aluminum alloys AA1060, *J. Coating Technol. Res.* 21 (3) (2023) 893–905, <https://doi.org/10.1007/s11998-023-00858-4>.
- [132] C. Lou, R. Zhang, X. Lu, C. Zhou, Z. Xin, Facile fabrication of epoxy/polybenzoxazine based superhydrophobic coating with enhanced corrosion resistance and high thermal stability, *Colloids Surf. A Physicochem. Eng. Asp.* 562 (2019) 8–15, <https://doi.org/10.1016/j.colsurfa.2018.10.066>.
- [133] C. Zhou, M. Fu, H. Xie, Y. Gong, J. Chen, J. Liu, Z. Xin, Polybenzoxazine/epoxy composite coatings: effect of crosslinking on corrosion resistance, *Ind. Eng. Chem. Res.* 60 (4) (2021) 1675–1683, <https://doi.org/10.1021/acs.iecr.0c05903>.
- [134] V. Selvaraj, T. Raghavarshini, M. Alagar, Development of Prosopis juliflora carbon-reinforced PET bottle waste-based epoxy-blended bio-phenolic benzoxazine composites for advanced applications, *RSC advances* 10 (10) (2020) 5656–5665, <https://doi.org/10.1039/C9RA08741A>.
- [135] W.A.W. Hassan, J. Liu, B.J. Howlin, H. Ishida, I. Hamerton, Examining the influence of bisphenol a on the polymerisation and network properties of an aromatic benzoxazine, *Polymer* 88 (2016) 52–62, <https://doi.org/10.1016/j.polymer.2016.01.041>.
- [136] X. Cao, G. Cai, Y. Wang, J. Pan, X. Zhang, Z. Dong, Bio-inspired polybenzoxazine coating: anti-corrosion and anti-abrasion performance enhancement through monomer design, *Prog. Org. Coating* 174 (2023) 107283, <https://doi.org/10.1016/j.porgcoat.2022.107283>.
- [137] D.M. Patil, G.A. Phalal, S.T. Mhaske, Enhancement of anti-corrosive performances of cardanol based amine functional benzoxazine resin by copolymerizing with epoxy resins, *Prog. Org. Coating* 105 (2017) 18–28, <https://doi.org/10.1016/j.porgcoat.2016.10.027>.
- [138] C. Zhou, X. Lu, Z. Xin, J. Liu, Y. Zhang, Hydrophobic benzoxazine-cured epoxy coatings for corrosion protection, *Prog. Org. Coating* 76 (9) (2013) 1178–1183, <https://doi.org/10.1016/j.porgcoat.2013.03.013>.
- [139] H. Ishida, D.J. Allen, Physical and mechanical characterization of near-zero shrinkage polybenzoxazines, *Journal of polymer science Part B: Polymer physics* 34 (6) (1996) 1019–1030, [https://doi.org/10.1002/\(SICI\)1099-0488\(19960430\)34:6<1019::AID-POLB1>3.0.CO;2-T](https://doi.org/10.1002/(SICI)1099-0488(19960430)34:6<1019::AID-POLB1>3.0.CO;2-T).
- [140] S. Elavarasan, N. Vijayakumari, D. Anbuselvi, Enhancing anticorrosive property of mild steel coated by synthesized eugenol-based benzoxazine with 3-acetyl phenyl side chain and copolymerizing with urethane, *RASAYAN Journal of Chemistry* 17 (4) (2024) 1957–1966, <https://doi.org/10.31788/rjc.2024.1748945>.
- [141] J. Chen, R. Jian, K. Yang, W. Bai, C. Huang, Y. Lin, B. Zheng, F. Wei, Q. Lin, Y. Xu, Urushiol-based benzoxazine copper polymer with low surface energy, strong substrate adhesion and antibacterial for marine antifouling application, *J. Clean. Prod.* 318 (2021) 128527, <https://doi.org/10.1016/j.jclepro.2021.128527>.
- [142] J. Chen, X. Zheng, R. Jian, W. Bai, G. Zheng, Z. Xie, Q. Lin, F. Lin, Y. Xu, In situ reduction of silver nanoparticles/urushiol-based polybenzoxazine composite coatings with enhanced antimicrobial and antifouling performances, *Polymers* 16 (8) (2024), <https://doi.org/10.3390/polym16081167>.
- [143] R.V. Gonçalves, I.Q. Liposki, L.W. Dias, A.F. Baldissera, M.R. da Silva Silveira, C. A. Ferreira, L. Bonnaud, N.R. de Souza Basso, Corrosion protection of benzoxazine and cardanol-doped polyaniline coatings, *J. Coating Technol. Res.* 19 (2) (2021) 575–586, <https://doi.org/10.1007/s11998-021-00545-2>.
- [144] L. Dumas, L. Bonnaud, M. Olivier, M. Poorteman, P. Dubois, High performance benzoxazine/CNT nanohybrid network – an easy and scalable way to combine attractive properties, *Eur. Polym. J.* 58 (2014) 218–225, <https://doi.org/10.1016/j.eurpolymj.2014.06.023>.
- [145] K. Zhang, Y. Liu, L. Han, J. Wang, H. Ishida, Synthesis and thermally induced structural transformation of phthalimide and nitrile-functionalized benzoxazine: toward smart ortho-benzoxazine chemistry for low flammability thermosets, *RSC advances* 9 (3) (2019) 1526–1535, <https://doi.org/10.1039/C8RA10009H>.

- [146] A. Mahdy, M.G. Mohamed, K.I. Aly, H.B. Ahmed, H.E. Emam, Liquid crystalline polybenzoxazines for manufacturing of technical textiles: water repellency and ultraviolet shielding, *Polym. Test.* 119 (2023) 107933, <https://doi.org/10.1016/j.polymertesting.2023.107933>.
- [147] Y. Wei, J. Chen, Y. Zhang, Z. Lu, Color changing Pickering emulsions stabilized by polysiloxane microspheres bearing phenolphthalein groups, *RSC advances* 5 (88) (2015) 71824–71829, <https://doi.org/10.1039/C5RA12453K>.
- [148] P. Thirukumaran, R. Sathiyamoorthi, A. Shakila Parveen, M. Sarojadevi, New benzoxazines from renewable resources for green composite applications, *Polym. Compos.* 37 (2) (2016) 573–582, <https://doi.org/10.1002/pc.23214>.
- [149] P. Thirukumaran, A. Shakila Parveen, M. Sarojadevi, Synthesis and copolymerization of fully biobased benzoxazines from renewable resources, *ACS Sustain. Chem. Eng.* 2 (12) (2014) 2790–2801, <https://doi.org/10.1021/sc500548c>.
- [150] E.I. Bîru, S.A. Gărea, H. Iovu, Developing polybenzoxazine composites based on various carbon structures, *Macromol. Chem. Phys.* 220 (3) (2019), <https://doi.org/10.1002/macp.201800322>.
- [151] V. Selvaraj, T.R. Raghavarshini, Building up of Prosopis juliflora carbon incorporated cardanol based polybenzoxazine composites with intensification of mechanical and corrosion resistance properties for adaptable applications, *Polym. Bull.* 77 (12) (2019) 6449–6466, <https://doi.org/10.1007/s00289-019-03084-4>.
- [152] E. Husain, T.N. Narayanan, J.J. Taha-Tijerina, S. Vinod, R. Vajtai, P.M. Ajayan, Marine corrosion protective coatings of hexagonal boron nitride thin films on stainless steel, *ACS applied materials & interfaces* 5 (10) (2013) 4129–4135, <https://doi.org/10.1021/am400016y>.
- [153] J. Wang, N. Wang, M. Liu, C. Ge, B. Hou, G. Liu, W. Sun, Y. Hu, Y. Ning, Hexagonal boron nitride/poly (vinyl butyral) composite coatings for corrosion protection of copper, *J. Mater. Sci. Technol.* 96 (2022) 103–112, <https://doi.org/10.1016/j.jmst.2021.03.075>.
- [154] Y. Tian, X. Zhang, Z. Su, J. Liu, H. Yang, M. Khalid, H. Xiao, P. Hu, Ultra-high-efficiency corrosion protection of metallic surface based on thin and dense hexagonal boron nitride coating films, *Langmuir* 40 (13) (2024) 7139–7146, <https://doi.org/10.1021/acs.langmuir.4c00272>.
- [155] S. Roy, X. Zhang, A.B. Puthirath, A. Meiyazhagan, S. Bhattacharyya, M. M. Rahman, G. Babu, S. Susarla, S.K. Sajju, M.K. Tran, Structure, properties and applications of two-dimensional hexagonal boron nitride, *Adv. Mater.* 33 (44) (2021) 2101589, <https://doi.org/10.1002/adma.202101589>.
- [156] J. Eichler, C. Lesniak, Boron nitride (BN) and BN composites for high-temperature applications, *J. Eur. Ceram. Soc.* 28 (5) (2008) 1105–1109, <https://doi.org/10.1016/j.jeurceramsoc.2007.09.005>.
- [157] Y. Zhou, Y. Wang, T. Liu, G. Xu, G. Chen, H. Li, L. Liu, Q. Zhuo, J. Zhang, C. Yan, Superhydrophobic hBN-regulated sponges with excellent absorbency fabricated using a green and facile method, *Sci. Rep.* 7 (1) (2017) 45065, <https://doi.org/10.1038/srep45065>.
- [158] A. Renaud, L. Bonnaud, L. Dumas, T. Zhang, Y. Paint, F. Fasano, O. Kulyk, E. Pospisilova, B. Nysten, A. Delcorte, D. Bonifazi, P. Dubois, M.-G. Olivier, M. Poorteman, A benzoxazine/substituted borazine composite coating: a new resin for improving the corrosion resistance of the pristine benzoxazine coating applied on aluminum, *Eur. Polym. J.* 109 (2018) 460–472, <https://doi.org/10.1016/j.eurpolymj.2018.10.018>.
- [159] C. Zhou, X. Lu, Z. Xin, J. Liu, Y. Zhang, Polybenzoxazine/SiO<sub>2</sub> nanocomposite coatings for corrosion protection of mild steel, *Corros. Sci.* 80 (2014) 269–275, <https://doi.org/10.1016/j.corsci.2013.11.042>.
- [160] S. Malathi Devi, D. Madhavan, K. Jeyasubramanian, A. Vimalraj, O.H. Gnanadhas Sobhin, Synergistic effect of activated carbon from disposed plastics and polybenzoxazine composite coating on corrosion inhibition, *Polym. Adv. Technol.* 35 (2) (2024), <https://doi.org/10.1002/pat.6321>.
- [161] M. Matandabuzo, D. Dovorogwa, *Activated carbons from waste tyre pyrolysis: application, in: Recent Perspectives in Pyrolysis Research, IntechOpen, 2022.*
- [162] C. Ge, D. Lian, S. Cui, J. Gao, J. Lu, Highly selective CO<sub>2</sub> capture on waste polyurethane foam-based activated carbon, *Processes* 7 (9) (2019) 592, <https://doi.org/10.3390/pr7090592>.
- [163] F. Hussin, M.K. Aroua, M.A. Kassim, U.F. Md Ali, Transforming plastic waste into porous carbon for capturing carbon dioxide: a review, *Energies* 14 (24) (2021) 8421, <https://doi.org/10.3390/en14248421>.
- [164] E.E. Özbaşa, B. Balçık, H. Ozcana, Preparation of activated carbon from waste tires, and its use for dye removal, *Desalin Water Treat* 172 (2019) 78–85, <https://doi.org/10.5004/dwt.2019.24493>.
- [165] D. Xu, C. Lou, J. Huang, X. Lu, Z. Xin, C. Zhou, Effect of inhibitor-loaded halloysite nanotubes on active corrosion protection of polybenzoxazine coatings on mild steel, *Prog. Org. Coating* 134 (2019) 126–133, <https://doi.org/10.1016/j.porgcoat.2019.04.021>.
- [166] S.V. Lamaka, B. Vaghefinazari, D. Mei, R.P. Petrauskas, D. Höche, M. L. Zheludkevich, Comprehensive screening of Mg corrosion inhibitors, *Corros. Sci.* 128 (2017) 224–240, <https://doi.org/10.1016/j.corsci.2017.07.011>.
- [167] Y. Cao, C. Chen, X. Lu, D. Xu, J. Huang, Z. Xin, Bio-based polybenzoxazine superhydrophobic coating with active corrosion resistance for carbon steel protection, *Surf. Coating. Technol.* 405 (2021), <https://doi.org/10.1016/j.surfcoat.2020.126569>.
- [168] M. Yadav, R. Sinha, S. Kumar, I. Bahadur, E. Ebenso, Synthesis and application of new acetohydrazide derivatives as a corrosion inhibition of mild steel in acidic medium: insight from electrochemical and theoretical studies, *J. Mol. Liq.* 208 (2015) 322–332, <https://doi.org/10.1016/j.molliq.2015.05.005>.
- [169] P. Singh, E.E. Ebenso, L.O. Olasunkanmi, I. Obot, M. Quraishi, Electrochemical, theoretical, and surface morphological studies of corrosion inhibition effect of green naphthyridine derivatives on mild steel in hydrochloric acid, *J. Phys. Chem. C* 120 (6) (2016) 3408–3419, <https://doi.org/10.1021/acs.jpcc.5b11901>.
- [170] S.K. Saha, A. Dutta, P. Ghosh, D. Sukul, P. Banerjee, Adsorption and corrosion inhibition effect of Schiff base molecules on the mild steel surface in 1 M HCl medium: a combined experimental and theoretical approach, *Phys. Chem. Phys.* 17 (8) (2015) 5679–5690, <https://doi.org/10.1039/C4CP05614K>.
- [171] A. Espinoza-Vazquez, F.J. Rodriguez-Gomez, I.K. Martinez-Cruz, D. Angeles-Beltran, G.E. Negron-Silva, M. Palomar-Pardave, L.L. Romero, D. Perez-Martinez, A.M. Navarrete-Lopez, Adsorption and corrosion inhibition behaviour of new theophylline-triazole-based derivatives for steel in acidic medium, *R. Soc. Open Sci.* 6 (3) (2019) 181738, <https://doi.org/10.1098/rsos.181738>.
- [172] K. Haruna, T.A. Saleh, M. Quraishi, Expired metformin drug as green corrosion inhibitor for simulated oil/gas well acidizing environment, *J. Mol. Liq.* 315 (2020) 113716, <https://doi.org/10.1016/j.molliq.2020.113716>.
- [173] B. Chambers, D. Gambale, Material selection in strong hydrogen sulfide acidizing environments, *Stainl. Steel World* 23 (2011) 29–35.